AD-A163 810 HOT GAS CORROSION OF SILICON BASED CERAMICS(U) OHIO STATE UNIV RESEARCH FOUNDATION COLUMBUS E R KREIDLER ET AL. 13 DEC 85 ARO-18141.2-MS 1/1

UNCLASSIFIED DAAG29-82-K-0149 F/G 11/2 NL

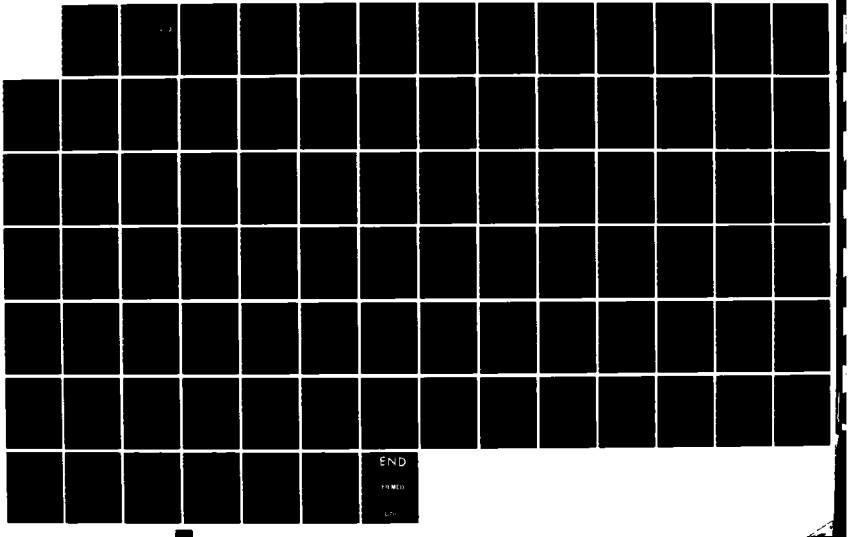

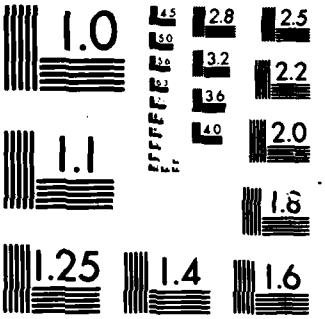

RF Project 763186/714674
Final Report

HOT GAS CORROSION OF SILICON BASED CERAMICS

Eric R. Kreidler and Dennis W. Readey
Department of Ceramic Engineering

For the Period
June 1, 1982 - September 30, 1985

DEPARTMENT OF THE ARMY
Army Research Office
P.O. Box 12211
Research Triangle Park, North Carolina 27709

Contract No. DAAG29-82-K-0149

December 1985

The view, opinions, and/or findings contained in this report are those of the authors and should not be construed as an official department of the Army position, policy, or decision, unless so designated by other documentation.

OSU
The Ohio State University Research Foundation
1314 Kinnear Road
Columbus, Ohio 43212

Unclassified

SECURITY CLASSIFICATION OF THIS PAGE (When Data Entered)

REPORT DOCUMENTATION PAGE		READ INSTRUCTIONS BEFORE COMPLETING FORM
1. REPORT NUMBER ARO 18141.2-MS	2. GOVT ACCESSION NO. ADA 163810	3. RECIPIENT'S CATALOG NUMBER
4. TITLE (and Subtitle) HOT GAS CORROSION OF SILICON BASED CERAMICS		5. TYPE OF REPORT & PERIOD COVERED Final Report 6/1/82 - 9/30/85
		6. PERFORMING ORG. REPORT NUMBER 714674/763186
7. AUTHOR(s) Eric R. Kreidler and Dennis W. Readey		8. CONTRACT OR GRANT NUMBER(s) DAAG29-82-K-0149
9. PERFORMING ORGANIZATION NAME AND ADDRESS The Ohio State University Research Foundation 1314 Kinnear Road Columbus, Ohio 43212-1194		10. PROGRAM ELEMENT, PROJECT, TASK AREA & WORK UNIT NUMBERS
11. CONTROLLING OFFICE NAME AND ADDRESS U. S. Army Research Office Post Office Box 12211 Research Triangle Park, NC 27709		12. REPORT DATE December 1985 13. NUMBER OF PAGES 85
14. MONITORING AGENCY NAME & ADDRESS(if different from Controlling Office)		15. SECURITY CLASS. (of this report) Unclassified 15a. DECLASSIFICATION/DOWNGRADING SCHEDULE

16. DISTRIBUTION STATEMENT (of this Report)

Approved for public release; distribution unlimited.

17. DISTRIBUTION STATEMENT (of the abstract entered in Block 20, if different from Report)

18. SUPPLEMENTARY NOTES

THE VIEW, OPINIONS, AND/OR FINDINGS CONTAINED IN THIS REPORT ARE THOSE OF THE AUTHOR(S) AND SHOULD NOT BE CONSTRUED AS AN OFFICIAL DEPARTMENT OF THE ARMY POSITION, POLICY, OR DECISION, UNLESS SO DESIGNATED BY OTHER DOCUMENTATION.

19. KEY WORDS (Continue on reverse side if necessary and identify by block number)

silicon carbide, silica,

20. ABSTRACT (Continue on reverse side if necessary and identify by block number)

The hot gas corrosion of (SiC) and (SiO_2) has been studied in a preliminary way, using two instruments constructed at The Ohio State University for this purpose. The two ceramics are not corroded by atmospheres containing 10% HCl in argon at temperatures up to 1150°C. However noticeable attack occurs in hydrogen at 1300°C when the water vapor pressure is below 10^{-5} atm. Most of the work on the project has concentrated on the construction and debugging of a high temperature, high pressure mass spectrometer sampling device to be used for quantitative studies of the chemistry and thermodynamics of corrosion (cont)

DD FORM 1 JAN 73 1473 EDITION OF 1 NOV 65 IS OBSOLETE

Unclassified

SECURITY CLASSIFICATION OF THIS PAGE (When Data Entered)

20. reactions. A high temperature thermogravimetric system has also been constructed to study the kinetics of the hot gas corrosion reactions. Theoretical calculations of the chemical equilibria, to be expected in a number of corrosion reactions, have been carried out and are included in the report.

HOT GAS CORROSION OF SILICON BASED CERAMICS

FINAL REPORT

ERIC R. KREIDLER

and

DENNIS W. READEY

DECEMBER 13, 1985

U. S. ARMY RESEARCH OFFICE

CONTRACT NO. DAAG29-82-K-0149

DEPARTMENT OF CERAMIC ENGINEERING
THE OHIO STATE UNIVERSITY

FOREWORD

The mass spectrometer sampling system and the thermogravimetric balance needed for corrosion studies on silicon based ceramics have been completed. Preliminary corrosion experiments have been conducted using both pieces of equipment. During the first two years, the greatest emphasis was placed on the design, construction and debugging of the mass spectrometer sampling system. This proved to be a more formidable job than first visualized, and a number of difficulties were encountered which we believe have mostly been solved. Therefore, although the mass spectrometer has been on line for about one year, due to the problems encountered, less experimental work on corrosion was completed than originally planned. We are continuing this work, using funds derived from the Department of Ceramic Engineering, and will seek renewal funding when feasibility of the technique has been demonstrated. The thermogravimetric balance was completed within the last six months and has yielded useful information on the corrosion of SiC in wet and dry hydrogen.

CONTENTS page

LIST OF APPENDICES, FIGURES AND TABLES

I. BODY OF REPORT

Much of the detailed technical content of this report will be found in Appendices A and B. However, a summary of the most important results and a section on the most recent work will be included herein.

A. Statement of the Problem Studied

There are two classes of corrosion mechanisms which can damage the materials used in the construction of gas turbines. One class deals with the attack of the materials by condensed films of molten salts such as sodium sulfate or sodium carbonate. Corrosion in such cases has been extensively studied[1-4] and the effects of such corrosion processes on the mechanical strength of materials have been determined[5,6]. Corrosion by molten salts can occur only if the saturated vapor pressure of the salts present in the combustion gases have been exceeded. At higher temperatures, such as are expected during steady state operation of a ceramic turbine, condensation of fused salts will not occur. In this case, corrosion by direct reaction of hot combustion gases with the turbine materials will be dominant. This is the hot gas corrosion problem that we have set out to study. The materials of interest in this study are the silicon based ceramics; silicon carbide (SiC), silicon nitride (Si_3N_4), and silica (SiO_2). The variables in the study are: gas temperature, pressure and composition; and ceramic type, purity, and density.

The work consists of thee integrated parts. The first part is to model the corrosion process by using the SOLGASMIX-PV computer code[7] to calculate the chemical equilibria in the system

of interest. The SOLGASMIX-PV program is based upon a free energy minimization scheme, and requires as input a complete list of reaction species and their free energies of formation. The program should give reliable results if the input thermodynamic data are reliable. However, since little is known about hot gas corrosion reactions in ceramics, the second part is to directly study the corrosion reaction in a suitable mass spectrometer. The objectives of this phase are to determine (a) what gaseous species are present in a given corrosion reaction and (b) the free energies of formation of these species. These data are then put back into the SOLGASMIX-PV program and an improved calculation is made. Comparisons of the experimental results and calculations are then done to see how well the thermodynamics of the corrosion process are understood. The calculations assume that chemical equilibrium has been established in the system. This assumption may not be true in a flowing gas stream, and consequently part three involves studies of the kinetics of the corrosion process. These studies are done in a sensitive thermogravimetric balance which can reproduce the conditions in the mass spectrometer sampling chamber. The kinetic data can be used to determine whether the rate limiting step in the corrosion process is diffusion controlled or surface reaction controlled. By combining the results of the thermodynamic studies done on the mass spectrometer with the kinetic experiments done on the thermogravimetric balance, the mechanism of corrosion can be understood in detail. The general strategy is to first understand the simplest corrosion reactions and then to introduce

additional species to more closely approximate the conditions actually found in turbine engines.

B. Summary of Important Results

The necessary equipment to carry out the experimental program outlined above has been constructed. The mass spectrometer system is described in detail in Appendix A, and the nature of the problems encountered and the steps taken to solve them have been indicated. The unique feature of the mass spectrometer is the ability to sample gaseous reaction products from high pressure and temperature environments in a way that minimizes the chance for chemical changes in the sampled gas. Preliminary experiments with the mass spectrometer indicate that SiC and SiO_2 are not significantly corroded in 10% HCl-Ar mixtures at 1 atm and temperatures up to 1150°C. The computer calculations (Appendix B) indicate that extensive reaction should occur with SiC under these conditions, but that SiO_2 reacts only to a limited extent. The discrepancy between experiment and calculations is due either to slow kinetics or to the presence of sufficient oxidizing species in the gas phase to prevent breakdown of the protective silica film. Further studies will be needed to determine which is the case.

Corrosion of SiC in dry and wet hydrogen at 1300°C has been studied with the thermogravimetric balance. As shown in Fig. 1, the reaction rate goes through a maximum at about 10^{-5} atm of water vapor pressure. As indicated in the following section (C.2.), the maximum is due to a transition from active to passive oxidation of silicon carbide by water vapor.

C. Recent Work

This section summarizes work done in the period from July 1, 1985 to November 30, 1985, which has not been previously reported. (Note that work from October 1, 1985 to November 30, 1985 was supported by the Department of Ceramic Engineering of The Ohio State University.)

1. Mass Spectroscopy

The major thrust of the experimental work conducted this quarter has dealt with the modification of the existing mass spectrometer sampling system to accommodate an open end tube furnace. This configuration offers certain advantages over the previously used flow reactor. These advantages include; easier system alignment, greater system stability, and easier exchange of test samples.

The main aspect of this transformation was the installation of a platinum sampling cone on the bottom of the sampling system in place of the flow reactor assembly. The sampling cone (obtained from the NASA-Lewis Research Center) contains an 8 mil orifice and is brazed to a stainless steel flange. A brass mounting flange was designed to mate the sampling orifice flange to the existing vacuum system. A schematic diagram of the new sampling system is shown in Appendix A, Fig.1.

A new furnace was also designed for use with the sampling configuration. This consists of a platinum wound high alumina furnace tube (1-1/2 inch I.D.) housed in an 8 inch diameter rolled sheet steel furnace shell. The furnace assembly is mounted on a vertically translatable furnace stand to allow for easy

sample placement and exchange. Vertical translation is performed using a 2-ton bottle jack centered below the furnace stand.

At this point in the research preliminary pumping tests have been performed on the system with the new sampling configuration in place. The system was pumped down by placing a stainless steel "cup" with an o-ring seal over the sampling orifice to isolate the system from the atmosphere. When the system was pumped to a sufficiently low pressure the cup was removed and the system was opened to the atmosphere. The resulting pressures are shown in Table I. These pressures are favorable and indicate that the present pumping system can adequately support the new sampling cone configuration.

Table I. System pressures with new platinum sampling cone.

	Stage I	Stage II	Mass Spectrometer
Roughing Pumps Only	20 mTorr	105 mTorr	170 mTorr
Diffusion Pumps*	1×10^{-5}	6.8×10^{-6}	3.2×10^{-6}
Open Orifice*	2×10^{-5}	1.8×10^{-5}	5.0×10^{-6}

* Values given in Torr.

A laboratory air spectrum was also obtained with the new sampling cone in place. This spectrum compares nicely with those reported earlier from tests conducted with a thinned 7 mil ruby orifice. In addition slight translations of the orifice resulted in a rapid decay of beam intensity, indicating good molecular beam formation.

Work currently in progress includes the mating of the new furnace to the new sampling system. Due to space constraints beneath the vacuum chamber, care is being taken in the design of the furnace stand and translation mechanism to avoid later problems in sample exchange. In addition a venting system is being designed to accommodate the leakage of toxic gases associated with the open end furnace design.

Following completion of these design and construction steps experimental work will begin in earnest. Tentative plans for the initial experiments are the reactions of Si and SiC in a 10% Cl_2-90% Ar environment. Equilibrium calculations performed on these systems indicate that significant amounts of volatile silicon chlorine compounds ($SiCl_x$, where x=1 to 4) are produced by these reactions. Therefore, these experiments are considered to be a good test for the experimental apparatus.

Following successful completion of the preliminary experiments, a variety of detailed experiments will be performed as outlined in the initial research proposal.

2. TGA Studies

The thermogravimetric apparatus (TGA) was completed during the autumn quarter, and some preliminary experiments were done on polycrystalline SiC samples (Hexaloy from Sohio). Thus far, emphasis has been put on the control of the equipment and the experimental conditions rather than generating extensive data. The experimental conditions important in this research are;

a. control and measurement of water vapor pressure (P H_2O)

b. stability of hang down wire

c. sample preparation

Several samples were run at T = 1300°C, H_2 flow rate = 900 cc/min and P H_2O from 1.6×10^{-5} to 3.0×10^{-4} atm., and the relationship between the rate of weight loss and the water vapor pressure was obtained.

Samples were cut from the sintered SiC, obtained from Sohio, with a diamond wafering blade. The samples were polished with diamond pastes ranging in size from one micron downward. According to the supplier, the samples had been sintered in nitrogen to near theoretical density (> 97.5 %). The final dimensions of the samples were about 1.2 cm x 1.1 cm x 0.07 cm. Samples were ultrasonically cleaned in acetone and stored in a desiccator until used in the TGA experiments.

The control and measurement of the water vapor pressures are extremely important in these experiments. To control the water vapor pressure, all the water vapor was first eliminated by passing hydrogen through 'Deoxo', drierite, and liquid nitrogen traps. Then controlled amounts of water vapor were added by passing the hydrogen through water. The water vapor pressure was measured with an oxygen sensor made of yttria stabilized zirconia. With this oxygen sensor, oxygen partial pressure was measured at a temperature much lower than the sample temperature (~ 740°C), and converted into the water vapor pressure. In this way, water vapor pressure could be measured and controlled precisely.

The molybdenum wire, used to suspend the samples, turned out to be stable only in dry hydrogen, i.e., when P $H_2O < 3.0 \times 10^{-4}$ atm. at T = 1300°C. When the water vapor pressure was larger

than this, the weight gain due to oxidation of the Mo wire was comparable to the weight loss due to the reaction of SiC with hydrogen and water vapor. This means that molybdenum is not suitable as a sample support wire in wet hydrogen. Single crystal Al_2O_3 fiber is believed to be suitable for this application.

Weight loss of the SiC sample in H_2 at T = 1300°C and H_2 flow rate = 900 cc/min was measured as a function of P H_2O. Ignoring the thickness of the sample, the rate of weight loss (flux) was calculated from the sample dimensions and measured weight losses. These results are plotted in Fig.1. The data are not highly accurate because the thicknesses of the samples were neither exactly the same nor thin enough to be ignored. But, the trend, i.e., lower weight loss at high and low water vapor pressure and higher weight loss at intermediate water vapor pressure, is obvious. This behavior is due to the transition from active to passive oxidation of SiC. At lower water vapor pressure, weight loss occurs both by the reduction of SiO_2 by H_2 to volatile SiO and by the active oxidation of SiC by H_2O. These two reactions can occur simultaneously so that the rate of weight loss increases as P H_2O increases. However, at sufficiently high water vapor pressures, the oxygen partial pressure (due to dissociation of water vapor) will exceed the equilibrium value for the reaction

$$SiO_2(s) + H_2(g) = SiO(g) + H_2O(g)$$

and the vaporization of silica will be suppressed. The resulting silica film will serve as a diffusion barrier to further attack of the silicon carbide and the rate of weight loss will decrease.

Scanning electron micrographs taken after the experiments indicate that attack occurs preferably on the grain boundaries and pores.

Future plans call for the generation of a large body of data on the reaction between SiC and hydrogen. In this work, sample size will be standardized and held to close tolerances, and the weight loss data will be collected under the following experimental conditions: temperature, from 1300°C to 1700 °C; water vapor pressure, from 1.6×10^{-5} atm. to 1.0×10^{-2} atm.; H_2 flow rate, from 500 cc/min to 2000cc/min. Surface composition before and after corrosion as well as surface morphology after corrosion will be studied to determine if the corrosion reaction is influenced by dissolved impurities and/or secondary phases.

D. List of All Publications and Reports Published

1. Dennis S. Fox and Eric R. Kreidler, "A Mass Spectrometer Sampling System for the Study of Hot Gas Corrosion of Ceramic Turbine Materials", submitted to Journal American Ceramic Soc., August, 1985.
2. Dennis S. Fox and Eric R. Kreidler, "A Mass Spectrometer Sampling System for Analysis of Hot Corrosion Products at High Temperatures", presented at 1983 Fall Meeting of the American Ceramic Soc., Nov.1, 1983, Columbus, OH., abstract in Amer. Ceram. Soc. Bulletin62 [9] 965 (1983).
3. Dennis S. Fox and Eric R. Kreidler, "Hot Gas Corrosion of Silica by Hydrogen Chloride", presented at 87th Annual Meeting of the American Ceramic Soc., May 8, 1985, Cincinnati, OH, abstract in Extended Abstracts American

Ceramic Society 87th Annual Meeting, pg. 38 (1985).

4. John E. Marra and Eric R. Kreidler, "Equilibrium Calculations for the Hot-Gas Corrosion of Si-Based Ceramics", presented at 87th Annual Meeting of the American Ceramic Soc., May 8, 1985, Cincinnati, OH, abstract in Extended Abstracts American Ceramic Society 87th Annual Meeting, pg. 49 (1985).

E. List of All Participating Scientific Personnel and Degrees Earned While Employed on the Project.

1. Eric R. Kreidler, Associate Professor of Ceramic Engineering, The Ohio State University.
2. Dennis W. Readey, Professor of Ceramic Engineering, The Ohio State University.
3. Dennis S. Fox, Graduate Research Associate, Master's Degree, June 1985.
4. John E. Marra, Graduate Research Associate, Passed Comprehensive Examinations, June 1985, will go direct for Ph.D.
5. Hyoun Ee Kim, Graduate Research Associate, Passed Comprehensive Examination, June, 1985.
6. Andrew J. Sherman, Undergraduate Assistant.
7. Mary Anne Hobson, Undergraduate Assistant.
8. Satinder K. Nayar, Undergraduate Assistant.

II. BIBLIOGRAPHY

1. R.E. Tressler, M.D. Meiser, and T. Yonushonis, J. Amer. Ceram. Soc. 59 [5,6] 278 (1976).
2. D.W. McKee and D. Chatterji, J. Amer. Ceram. Soc. 59 [9,10] 442 (1976).
3. N.S. Jacobson and J.L. Smialek, J. Amer. Ceram. Soc. 68 [8] 432 (1985).
4. W.C. Bourne and R.E. Tressler, Bull Amer. Ceram. Soc. 59 443 (1980).
5. J.E. Siebels, Ceramics for High Performance Applications III. Reliability, pg. 793, ed. J. Burke, A.E. Gorum and R.N. Katz, Plenum Press 1983.
6. J.L. Smialek and N.S. Jacobson, NASA Technical Memorandum 87052, NASA Lewis Research Center 1984.
7. T.M. Besmann, Oak Ridge National Laboratory, TM-5775, (1977).

Also see references in Appendices A and B.

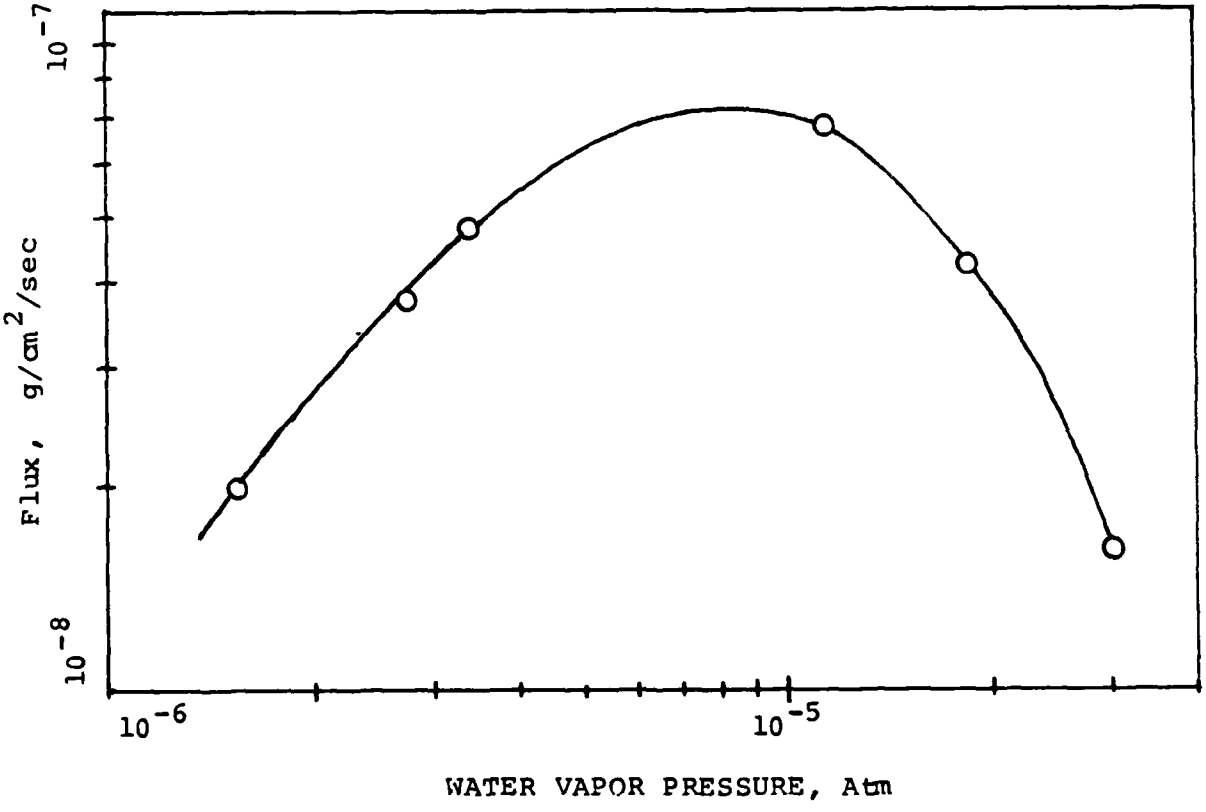

Fig. 1. Corrosion of SiC in wet hydrogen.

III. APPENDICES

APPENDIX A

A Mass Spectrometer Sampling System for the Study of Hot Gas Corrosion of Ceramic Turbine Materials.

A paper submitted to
The American Ceramic Society
in August, 1985
for publication

A Mass Spectrometer Sampling System for the Study of Hot Gas Corrosion of Ceramic Turbine Materials

D.S. Fox*+ and E.R. Kreidler*

Department of Ceramic Engineering

The Ohio State University, Columbus, Ohio

ABSTRACT

A high temperature mass spectrometer sampling system, capable of operating at atmospheric pressure, is being developed for studies of hot gas corrosion of ceramic turbine materials. Preliminary tests show that design goals have been met so far as pumping capabilities are concerned, however practical problems of obtaining thin small orifices in ceramic sample tubes are still under investigation. Initial corrosion experiments show that SiC and SiO_2 are not appreciably attacked by 10% HCl-90% argon atmospheres at temperatures up to 1150°C.

INTRODUCTION

Research into the development of ceramic materials for use in advanced heat engines has been conducted since about 1970.[1] These engines would have many advantages over similar engines based on nickel-chrome alloys. The higher operating temperatures that the ceramics can withstand will increase the thermal efficiency of the engine. The lower density of the ceramic engine materials will permit a greater power to weight ratio.

Presented at the 87th Annual Meeting of the American Ceramic Society, Cincinnati, OH, May 8, 1985 (No. 142-B-85).

* Member, the American Ceramic Society

+ Currently at NASA Lewis Research Center, Cleveland, OH.

Another advantage is that materials such as silicon carbide and silicon nitride are highly oxidation resistant due to the protective silica layer present on their surfaces.

A ceramic based engine must withstand severe operating conditions. The engine materials must endure intense mechanical and thermal stresses. In addition, the engine components are exposed to oxidizing or corrosive combustion gases. These gases can react with the engine materials to produce surface flaws that cause strength reduction and eventually catastrophic failure.[2]

The mechanisms of the corrosion reactions between hot combustion gases and ceramic materials such as silicon carbide and silicon nitride are not well known. In these systems, there are many possible reaction products. This paper describes an analytical apparatus which can be used to identify the corrosion products. The apparatus consists of a differentially pumped vacuum system used to create a supersonic beam of the sample gas and a mass spectrometer used to identify the chemical species produced during hot gas corrosion. The corrosion reaction is conducted in a flow reactor.

Hot gas corrosion of turbine engine materials usually occurs at pressures greater than atmospheric. Mass spectrometers, on the other hand, are low pressure instruments operated at 10^{-4} Pa (10^{-6} torr) or less. Therefore, to analyze reaction products generated at one atmosphere with a mass spectrometer, the pressure of the gas sample must be reduced by nine orders of magnitude. At the same time, the gas must retain the chemical composition found in the original sample. A technique that can be used to accomplish both objectives is free jet expansion.

When a gas flows through a small, knife edged orifice into a low pressure region, the gas expands into a free jet. The gas history (the change in pressure, density and temperature with time or distance) may be approximated by assuming an isentropic expansion.[3] This expansion is terminated by an abrupt transition to collisionless flow. If the gas is collimated, a molecular beam is created. The dimensions of the sampling orifice determine the type of gas flow through the opening. The orifice Knudsen number, Kn, is described by

$$Kn = x/D \qquad (1)$$

where x is the mean free path length of the gas molecules and D is the orifice diameter. If Kn is greater than ten, the flow through the orifice is effusive. The Knudsen cell sampling system commonly used with mass spectrometers is based on this type of flow. If Kn is less than 10^{-2}, the gas expands by continuum flow (dominated by collisions) and eventually forms a supersonic jet.

The formation of the supersonic molecular beam can be explained with basic thermodynamics. As the gas flows through the orifice and into the continuum flow region, the random thermal energy (enthalpy) of the colliding molecules is changed to directed kinetic energy, and adiabatic cooling of the gas occurs. As the expansion continues, the temperature and density of the gas are reduced until an essentially collisionless molecular flow is created. Stearns et al.[4] studied the expansion history of argon through a 0.025 cm diameter orifice and found that after six microseconds, the temperature of the gas (T_o = 300°K) had dropped to 10^{-2} T_o, the number density had fallen to

10^{-3} N_o, and the pressure had decreased to 10^{-5} P_o, where the subscript "o" represents conditions of the source gas before expansion. Any chemical reactions occurring in the sample gas will cease after expansion into the collisionless flow regime. The gaseous species downstream of the orifice will therefore remain, for all practical purposes, at their initial concentration.

Kantrowitz and Grey[5] did the pioneering work on the creation of high intensity molecular beams from gases undergoing free jet expansion. Their technique involved the placement of a slit, herein referred to as the skimmer, in the center of flow of the expanding gas. The formation of the molecular beam requires that several conditions be satisfied. First, the expansion of the gas from the sampling orifice to the skimmer entrance is isentropic in the continuum flow regime. Second, the flow at the skimmer is uniform and parallel to the skimmer and is undisturbed by its presence. Third, no molecular collisions can occur downstream of the skimmer entrance. Many investigators have constructed high pressure sampling systems based on the work of Kantrowitz and Grey and a number have coupled the system with a mass spectrometer.[4,6-9]

SYSTEM DESIGN

A cross section of the high pressure sampling system constructed at The Ohio State University is shown in Fig. 1. The system consists of two vacuum chambers used to step down the pressure from 101.3 kPa (760 torr) at the source to approximately 10^{-4} Pa (10^{-6} torr) so that the sample can be analyzed with a

time of flight mass spectrometer.* Each vacuum chamber has its own diffusion and roughing pumps. The working pressure in the first stage is approximately 0.1 Pa (10^{-3} torr) and in the second stage is 10^{-3} Pa (10^{-5} torr).

For pumping tests with gases at room temperature, the sampling orifice consists of a jeweler's ruby watch bearing attached to a brass flange with epoxy cement. The bearing is a thin disk with a small hole at its center that serves as the sampling orifice. Three different diameter orifices were used: 0.025 cm, 0.018 cm and 0.013 cm. The distance between the sampling orifice and the skimmer opening can be set at 1.27, 1.91 or 2.54 cm using the proper spacer ring. Stearns et al.[4] observed that the intensity of the supersonic beam is a function of the orifice to skimmer distance and that optimum intensities occur when this distance is approximately 100 times the orifice diameter.

The skimmer is placed in a position where it will intercept the free jet and allow the central core to travel into Stage II. The body of the skimmer is formed as a truncated cone having an apex angle of 60° and walls 0.32 cm thick. A small molecular beam skimmer cone** is clamped into place at the end of the skimmer body. The cone is constructed of copper, has walls 0.008 cm thick and has a circular opening at its apex 0.076 cm in diameter.

After the central core of the free jet passes through the

---

* Bendix model 3012, Cincinnati, OH.

** Beam Dynamics, Inc., Minneapolis, MN.

skimmer opening, it encounters a collimator. The purpose of the collimator is to decrease background noise caused by molecules scattered out of the beam. The collimator is a cone having an apex angle of 120° and walls 0.32 cm thick. A rectangular opening 0.18 cm by 0.53 cm is formed in the end of the collimator. A chopper* is mounted just ahead of the collimator opening. By chopping the molecular beam and using a technique known as lock-in detection[10], the low intensity molecular beam signals can be extracted from random background noise. The signal of interest is the ion current produced when the sample gas is ionized in the mass spectrometer.

The product species from the hot gas corrosion reactions are introduced into the high pressure sampling system via the flow reactor shown in Fig. 2. The reactor is mounted beneath the skimmer in place of the ruby sampling orifice. The flow reactor consists of a small ceramic tube, closed on one end, which contains the sample and has arrangements for introducing reactant gases of controlled composition and pressure. The flow tube is placed inside a tube furnace capable of temperatures as high as 1500°C. The gas passes through the flow tube at a constant rate and reacts with the sample. The gaseous corrosion products then flow through a 0.025 cm diameter sampling orifice in the "closed" end of the tube. The orifice was made by ultrasonic drilling. There are provisions that allow vertical translation of the flow tube so the orifice to skimmer distance can be varied.

---

* Frequency Control Products, Inc., Woodside, NY.

EXPERIMENTAL RESULTS AND DISCUSSION

The initial experiments were done to determine the overall performance of the vacuum pumps. Gases at room temperature were introduced into the system through ruby orifices and the pressures in the sampling system and the mass spectrometer were measured with Bayard-Alpert type ion gauges*. The flow rate through the sampling orifice was measured with standard rotameters. The four variables in these tests were orifice size, orifice to skimmer distance, gas type and source pressure. The three sizes of ruby orifices and the three orifice to skimmer distances described above were used. Argon, nitrogen and hydrogen were sampled at source pressures of 20.3, 50.7, and 101.3 kPa (1/5, 1/2 and 1 atm). Representative results of these experiments are given in Figs. 3 to 6 and in Table I.

The maximum gas flow rate (Q) through a thin orifice, separating two chambers at pressures P_1 and P_2, occurs when the ratio $P_2/P_1 < 0.5$. Under these conditions the gas passes through the orifice at the velocity of sound and the flow rate is not affected by changes in P_2. Since the measured pressure ratio in this system is about 10^{-5}, the maximum flow rate will be obtained. The flow rate is given by the expression[11]

$$Q = P_1 A[\gamma kT/m]^{1/2}[2/(\gamma+1)]^{(\gamma+1)/2(\gamma-1)} \qquad (2)$$

where γ is the ratio of specific heats (C_p/C_v) of the gas, m is the mass of the gas molecule, k is Boltzmann's constant, T is temperature, and A is orifice area. For nitrogen at 293 K and 101.3 kPa (1 atm) the equation reduces to

$$Q = 1.58\ D^2 \qquad (3)$$

---

* Veeco Instruments, Inc., Plainview, NY.

where Q is in cubic meters per second and D (the orifice diameter) is in meters. The calculated flow rates for the three orifice sizes are compared to measured values in Table I. Although close, the measured values are consistently lower than the calculated values. The discrepancy may be attributed to the thickness of the ruby orifices. The calculations are for orifices with zero thickness, and as the the orifice becomes thicker it offers more resistance to gas flow thereby reducing the flow rate. As will be shown later, the thickness of the orifices causes problems in molecular beam formation.

Typical system pressures obtained with the ruby orifices are shown in Fig. 3. From these data it can be concluded that the pressures in each part of the instrument are sufficiently low to provide; good molecular beam formation, proper operation of the diffusion pumps, and proper operation of the mass spectrometer.

The effect of source pressure on the system is shown in Fig. 4. The rapid increase in stage I pressure, for source pressures exceeding 70.0 kPa, indicates that the first stage diffusion pump is beginning to choke due to an overload of gas. Therefore, at room temperature and atmospheric pressure, a 0.025 cm orifice is the largest that can be used. Choking of the diffusion pump was not observed under any conditions when pumping nitrogen or argon through the 0.013 and 0.018 cm orifices. However, when pumping hydrogen at atmospheric pressure, the 0.018 cm orifice showed some evidence of choking and the 0.025 cm orifice yielded such high pressures that it could not be used.

The effect of gas viscosity on system pressures was studied and the results are shown in Fig. 5. As would be expected, all

system pressures were inversely proportional to the gas viscosity. From this figure it is reasonable to conclude that air, argon, nitrogen, oxygen, etc. will behave similarly in the sampling system and that one orifice size will suffice for all. The less viscous gases such as hydrogen and helium will require a smaller orifice to prevent overloading of the pumps.

The effect of orifice to skimmer distance on system pressures is shown in Fig. 6. The stage I and stage II pressures increase as the orifice to skimmer distance decreases. The increase in stage I pressure is due to a reduction in the conductance of the vacuum chamber in the vicinity of the skimmer and orifice as the two are brought closer together. The increase in stage II pressure is due to the fact that at shorter distances the skimmer is intercepting a denser part of the free jet. The pressure in the mass spectrometer shows a maximum at an orifice to skimmer distance of about 100 D (i.e. 1.8 cm), which is in agreement with previous work[4].

Preliminary corrosion experiments were conducted on silica, silicon carbide and zinc oxide ceramics.

The silica sample was optical quality fused quartz*. A cube 1.0 cm on a side was cut and polished on 400 grit silicon carbide paper. The specimen was weighed and measured, then cleaned with a detergent solution and rinsed with distilled water and methanol. The sample was supported in the flow reactor atop a platinum-platinum 10% rhodium thermocouple. The system was pumped out, pure argon was admitted and the temperature was raised to 1000°C. Upon reaching the desired temperature, the

* Vitreosil, Thermal American Fused Quartz Co., Montville, NJ.

argon flow was replaced by a mixture of 90% argon 10% HCl while the mass spectrometer was operating. Mass spectra were obtained at 1000, 1050, 1100, and 1150°C. The mass spectra failed to show any evidence of corrosion products. Weights taken at the conclusion of the experiment confirmed that no corrosion had taken place.

Equilibrium calculations, using the SOLGASMIX-PV program [12], indicated that SiC should react more extensively than SiO_2 in an HCl containing atmosphere. Therefore, the next experiments were run with a specimen of silicon carbide*. The sample configuration and experimental conditions were the same as in the silica experiments. Calculations indicate that at 1150°C the equilibrium vapor pressure of $SiCl_4$ over SiC is 14.2 kPa whereas that over silica is 0.037 kPa. Again, however, the mass spectra failed to reveal any corrosion products. The sensitivity of the instrument is sufficient to detect as little as 0.03% (0.040 kPa) of $SiCl_4$ in the carrier gas. If the reaction were occurring to the extent indicated by the equilibrium calculations, the corrosion products would easily be detected. The samples were weighed after several hours at 1150°C in the argon-HCl mixture and showed a very small weight gain. Apparently traces of oxygen and/or water vapor in the gas stream resulted in some oxidation of the specimen. From this and the preceding experiment it is apparent that the kinetics of the reactions are much too slow to allow measureable corrosion under the conditions studied. The kinetics will be faster at higher temperatures, however, these

* NC203, Norton Co., Worcester, MA.

studies were limited to 1150°C because the flow reactor had a silica sample tube. Higher temperatures would result in viscous deformation and devitrification of the tube, which must be prevented to avoid damage to the skimmer. Alumina and silicon carbide reactor tubes will be used in future experiments.

Because of the temperature limitations of the equipment, zinc oxide was selected as a model system for study. Corrosion of zinc oxide by hydrogen is known to occur rapidly at temperatures below 1000°C. The products from this corrosion process are zinc vapor and water vapor. Reagent grade ZnO powder was pressed into pellets 1.3 cm in diameter by 1.0 cm high. The pellets were sintered in air at 800°C for 15 h to give them adequate strength for handling. The density of the pellets was 90% of theoretical. After weighing, the samples were loaded into the flow reactor. Since platinum is damaged by zinc vapor, the samples were supported on chromel-alumel thermocouples. Two experiments were conducted. In the first, the temperature was increased to 1000°C while the flow tube was kept under vacuum. Once the temperature stabilized, dry hydrogen was admitted at a source pressure of 101.3 kPa and mass spectra were obtained. In the second experiment, hydrogen was admitted while the sample was at room temperature. The temperature was increased to 1000°C at a rate of 20°C/min. Mass spectral scans were made at 50°C intervals beginning at 800°C. Weight measurements after the experiments showed that the samples lost about 30% of their weight, yet no reaction products were seen in the mass spectra. This was at first perplexing, but further analysis of the experiments revealed two problems; (a) the orifice channel length

(thickness) was too long which resulted in excessive gas scattering and prevented molecular beam formation and (b) the orifice became plugged with deposits of zinc metal and zinc oxide. The latter was most severe at the highest sample temperature (1000°C) and occurred because the orifice in the flow reactor was at a lower temperature than the sample, thus allowing condensation of the reaction products. An auxiliary heater is being incorporated into the flow reactor to prevent this.

Although the orifice eventually became plugged, it did remain open long enough for detection of zinc vapor, if a suitable molecular beam had formed. Since zinc and water vapor condense on the cool surfaces of the vacuum chamber, they will not be detected in the mass spectrometer if excessive scattering prevents molecular beam formation. Argon, being noncondensable, will be detected in either case. There were several pieces of evidence for poor beam formation with the flow reactor; (a) the chopped beam showed only a weak "in phase" signal when pure argon was flowing through the reactor, (b) the argon signal intensity was not proportional to the source pressure, and (c) the signal intensity was not affected by lateral translation of the orifice. All of these observations indicate that most of the signal was due to scattered argon background and that very little of it was due to an argon beam. This conclusion was confirmed by polishing one of the 0.018 cm ruby bearings until the channel length of the orifice was about 0.002 cm. Tests with this orifice gave good beam formation. As shown in Fig. 7 the argon signal intensity was proportional to source pressure up to source pressures of 55.0 kPa. After that the signal began to level off. These

observations are in agreement with results published by Stearns et al. The polished ruby orifice also yielded strong "in phase" signals when the beam was chopped and the intensity fell off rapidly as the orifice was laterally translated off the axis of the sampling system. These tests indicate that channel length of the orifices is critical to good beam formation, and that the channel length should not be longer than about 0.002 cm. The as received ruby bearings and the drilled flow reactor tubes had channel lengths about ten times longer. Means of machining holes 0.018 cm diameter by 0.002 cm long into the ends of alumina and silicon carbide tubes are now under study.

An alternative to using a flow reactor is to directly attach a platinum-rhodium sampling cone to the system as shown in Fig. 1. The sampling orifice is machined into the apex of the cone. The cone is then inserted into the end of a small tube furnace which contains the sample and the corrosive gas atmosphere. Equipment for implementing this sampling scheme is now being built. The design specifications for metal and ceramic orifices are the same, but are easier to realize in the more machineable metals.

CONCLUSIONS

Although hot gas corrosion products from ceramics have not yet been observed, an apparatus has been constructed which meets the pumping requirements for such work. The main problem, remaining to be solved, is the production of flow reactor tubes or platinum-rhodium sampling cones with suitable orifices. Several routes to obtaining these items are under investigation. Beam

formation and pumping tests both indicate that when proper orifices are obtained, the equipment will be suitable for hot gas corrosion studies on ceramics.

Preliminary experiments have shown that the corrosion of SiC and SiO_2 at 1150°C in an argon-HCl atmosphere is kinetically unfavorable, and that corrosion does not occur to a measureable extent under these conditions.

ACKNOWLEDGMENTS

The authors gratefully acknowledge support of this work by the U. S. Army Research Office, Research Triangle Park, North Carolina under contract No. DAAG29-82-K00149. The equilibrium calculations were done by Mr. John E. Marra, a Ph. D. candidate in Ceramic Engineering at The Ohio State University.

REFERENCES

[1]D.R. Johnson, A.C. Schaffhauser, V.J. Tennery, E.L. Long, Jr., and R.B. Schulz, "Ceramic Technology for Advanced Heat Engines Project," Am. Cer. Soc. Bull., 64 [2] 276-280 (1985).

[2]D.W. Richerson, "Evolution in the U.S. of Ceramic Technology for Turbine Engines," Am. Cer. Soc. Bull., 64 [2] 282-286 (1985).

[3]T.A. Milne and F.T. Greene, Advances in High Temperature Chemistry; Vol. 2, pp. 107-150, ed. L. Eyring, Academic Press, New York, 1969.

[4]C.A. Stearns, F.J. Kohl, G.C. Fryburg, and R.A. Miller, "A High Pressure Modulated Molecular Beam Mass Spectrometric Sampling System," NASA Technical Memorandum 73720; National Technical Information Service, Springfield, 1977.

[5]A. Kantrowitz and J. Grey, "A High Intensity Source for the Molecular Beam. Part I. Theoretical," Rev. Sci. Instr., 22 [5] 328-332 (1951).

[6]W.L. Fite and R.T. Brackman, "Collisions of Electrons with Hydrogen Atoms. I. Ionization," Phys. Rev., 112 [4] 1141-1151 (1958).

[7]F.T. Greene and T.A. Milne, "Mass Spectrometric Sampling of High Pressure-High Temperature Sources," pp. 841-850 in Advances in Mass Spectrometry; Vol. 3, The Institute of Petroleum, London, 1966.

[8]F.T. Greene, J. Brewer, and T.A. Milne, "Mass Spectrometric Studies of Reactions in Flames. I. Beam Formation and Mass Dependence in Sampling 1-Atm Gases," J. Chem. Phys., 40 [6] 1488-1495 (1964).

[9]D. Golomb, R.E. Good, and R.F. Brown, "Dimers and Clusters in Free Jets of Argon and Nitric Oxide," J. Chem. Phys., 52 [3] 1545-1551 (1970).

[10]S. Yamamoto and R.E. Stickney, "Analysis of "Lock-In" Detection of Modulated Molecular Beams Scattered from Solid Surfaces," J. Chem. Phys., 47 [3] 1091-1099 (1967).

[11]R. Loevinger, Vacuum Equipment and Techniques, pp. 16-20, ed. A. Guthrie and R. K. Wakerling, McGraw Hill, New York, 1949.

[12]T. M. Besmann, "SOLGASMIX-PV, a Computer Program to Calculate Equilibrium Relationships in Complex Chemical Systems", Oak Ridge National Laboratory, Technical Memorandum-5775, Oak Ridge, TN, 1977.

Table I. Nitrogen Flow Rates Through Ruby Orifices.

Orifice Diameter (m)	Flow Rates (m^3/s)	
	calculated	measured*
0.00013	2.56×10^{-6}	$2.1 \pm 0.6 \times 10^{-6}$
0.00018	5.01×10^{-6}	$4.1 \pm 0.2 \times 10^{-6}$
0.00025	10.23×10^{-6}	$6.5 \pm 0.4 \times 10^{-6}$

* Average of three measurements ± standard deviation. The gas was at 293 K and 101.3 kPa.

FIGURE CAPTIONS

Fig. 1. Cross section of sampling system.

Fig. 2. Cross section of flow reactor. T. C. indicates thermocouple.

Fig. 3. System pressures as a function of orifice size. In this and succeeding figures P_o is source pressure, S is orifice to skimmer distance and D is orifice diameter.

Fig. 4. System pressures as a function of source pressure.

Fig. 5. System pressures as a function of gas viscosity.

Fig. 6. System pressures as a function of orifice to skimmer distance.

Fig. 7. Argon ion intensity as a function of source pressure.

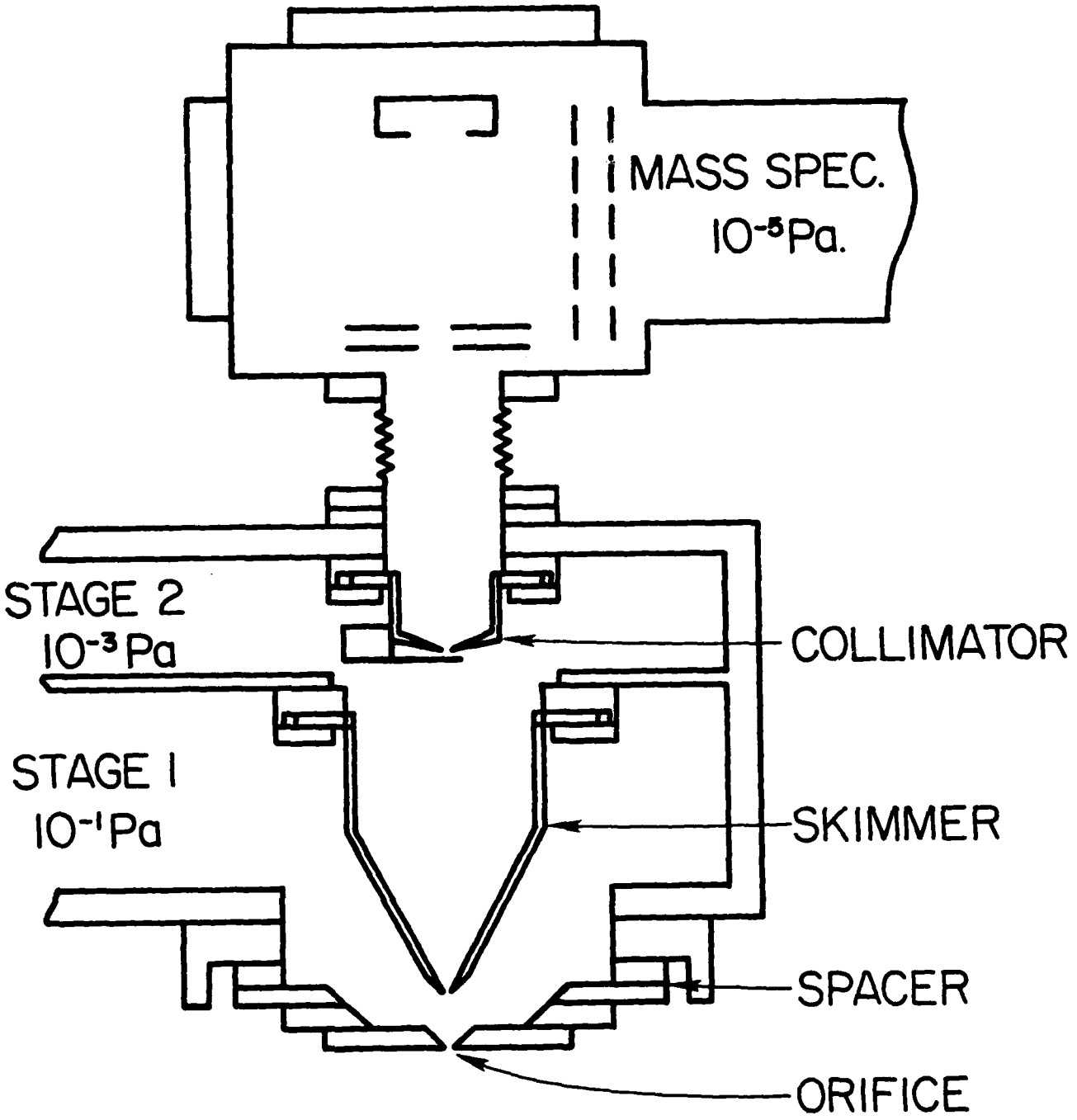
MASS SPEC.
10^{-5}Pa.
STAGE 2
10^{-3}Pa
COLLIMATOR
STAGE 1
10^{-1}Pa
SKIMMER
SPACER
ORIFICE

FIG. 1

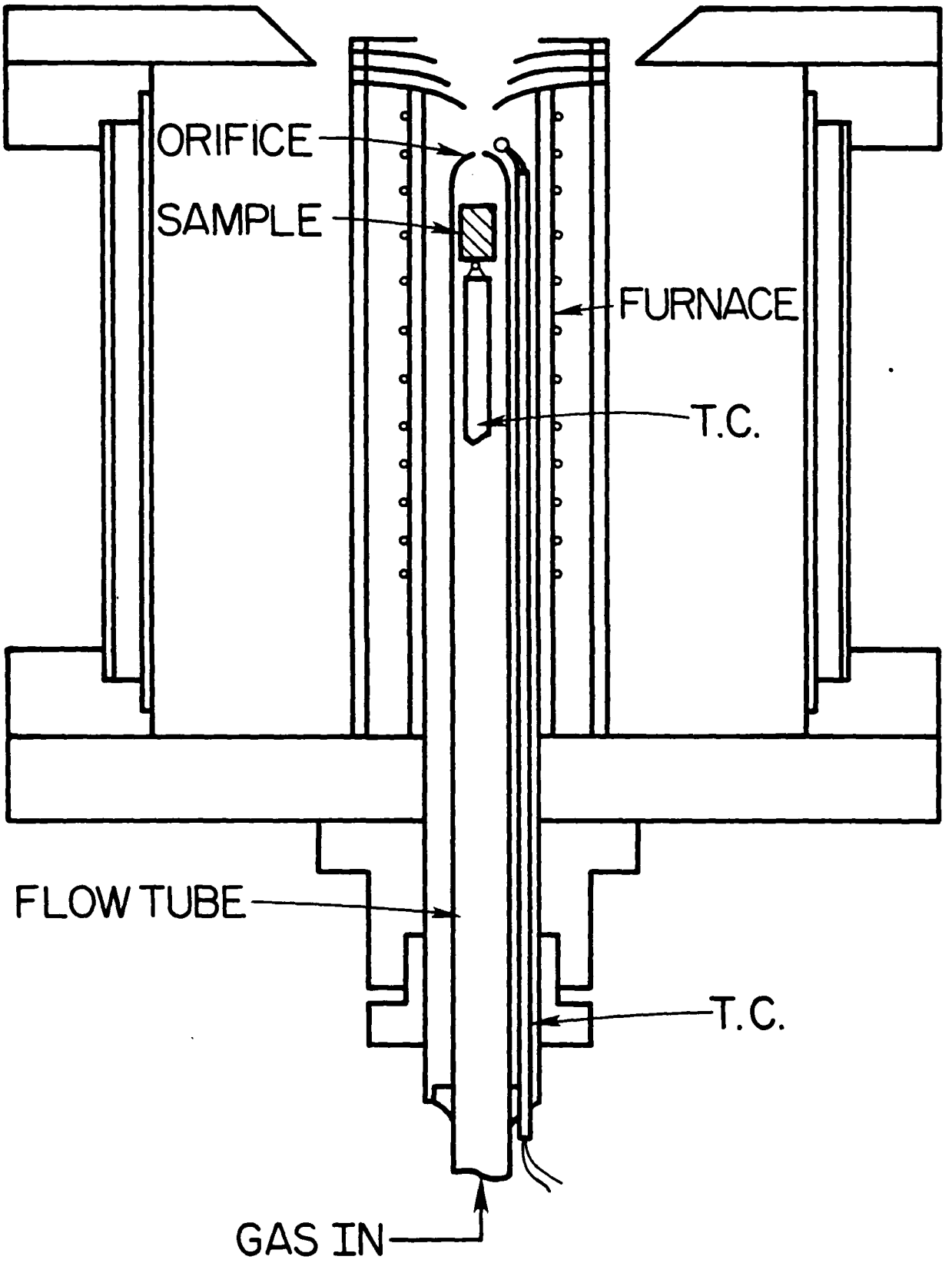

FIG. 2

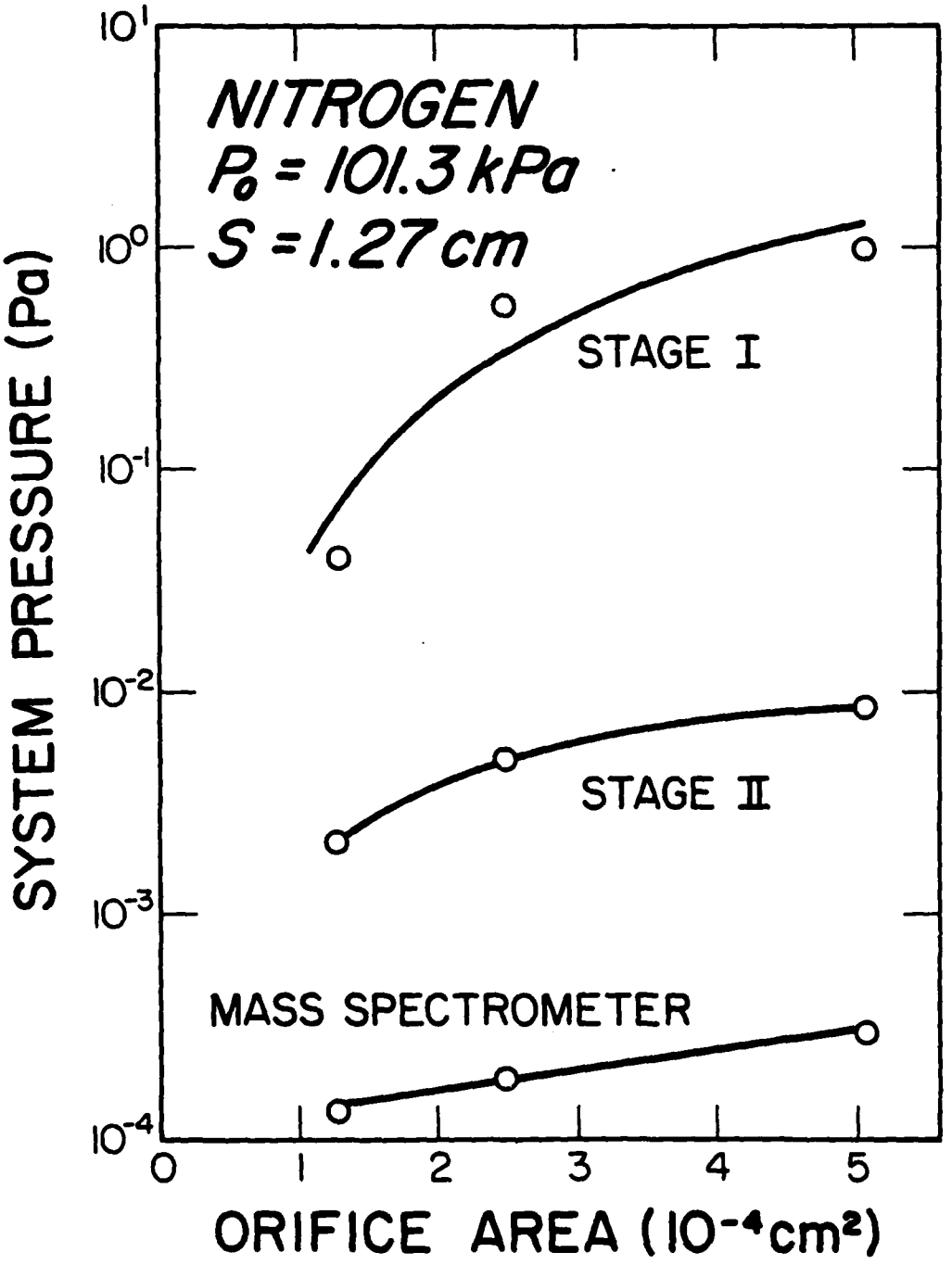
NITROGEN
P_o = 101.3 kPa
S = 1.27 cm
STAGE I
STAGE II
MASS SPECTROMETER
SYSTEM PRESSURE (Pa)
10^1
10^0
10^{-1}
10^{-2}
10^{-3}
10^{-4}
0
1
2
3
4
5
ORIFICE AREA (10^{-4}cm^2)

FIG. 3

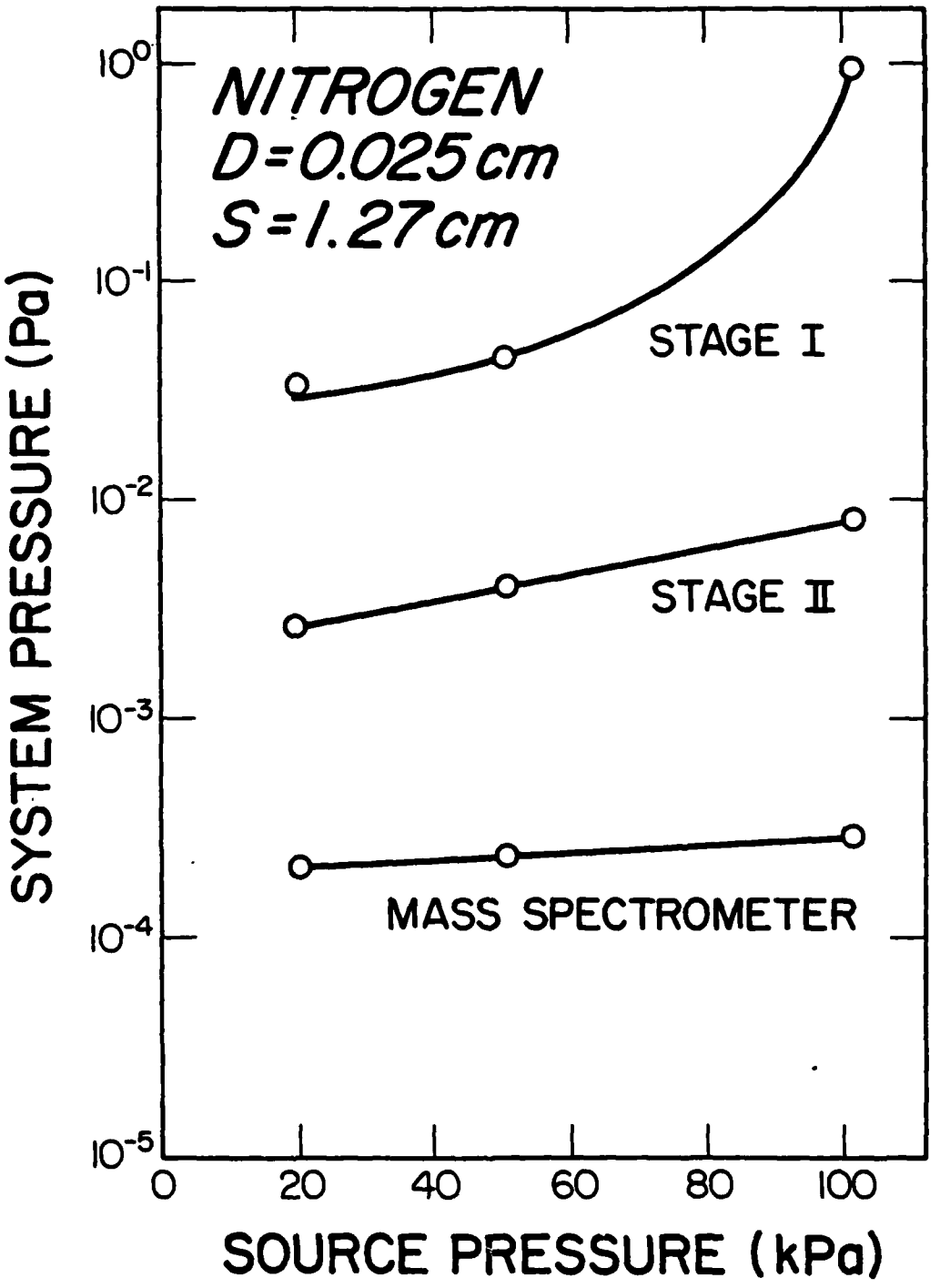
NITROGEN
D=0.025cm
S=1.27cm
STAGE I
STAGE II
MASS SPECTROMETER
SYSTEM PRESSURE (Pa)
10^0
10^-1
10^-2
10^-3
10^-4
10^-5
0
20
40
60
80
100
SOURCE PRESSURE (kPa)

FIG. 4

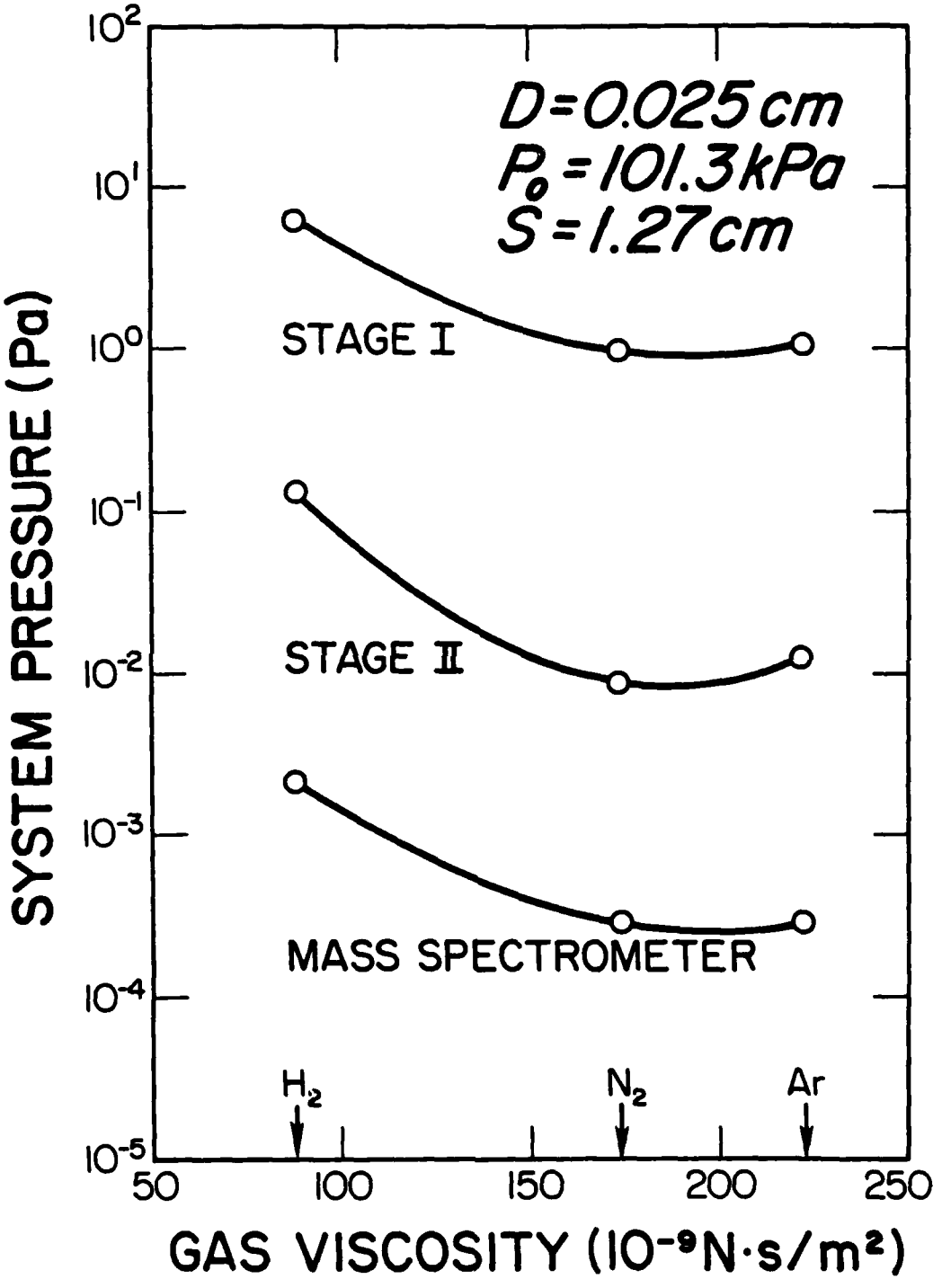
D=0.025cm
P₀=101.3kPa
S=1.27cm
STAGE I
STAGE II
MASS SPECTROMETER
SYSTEM PRESSURE (Pa)
10²
10¹
10⁰
10⁻¹
10⁻²
10⁻³
10⁻⁴
10⁻⁵
H₂
N₂
Ar
50
100
150
200
250
GAS VISCOSITY (10⁻⁹N·s/m²)

FIG. 5

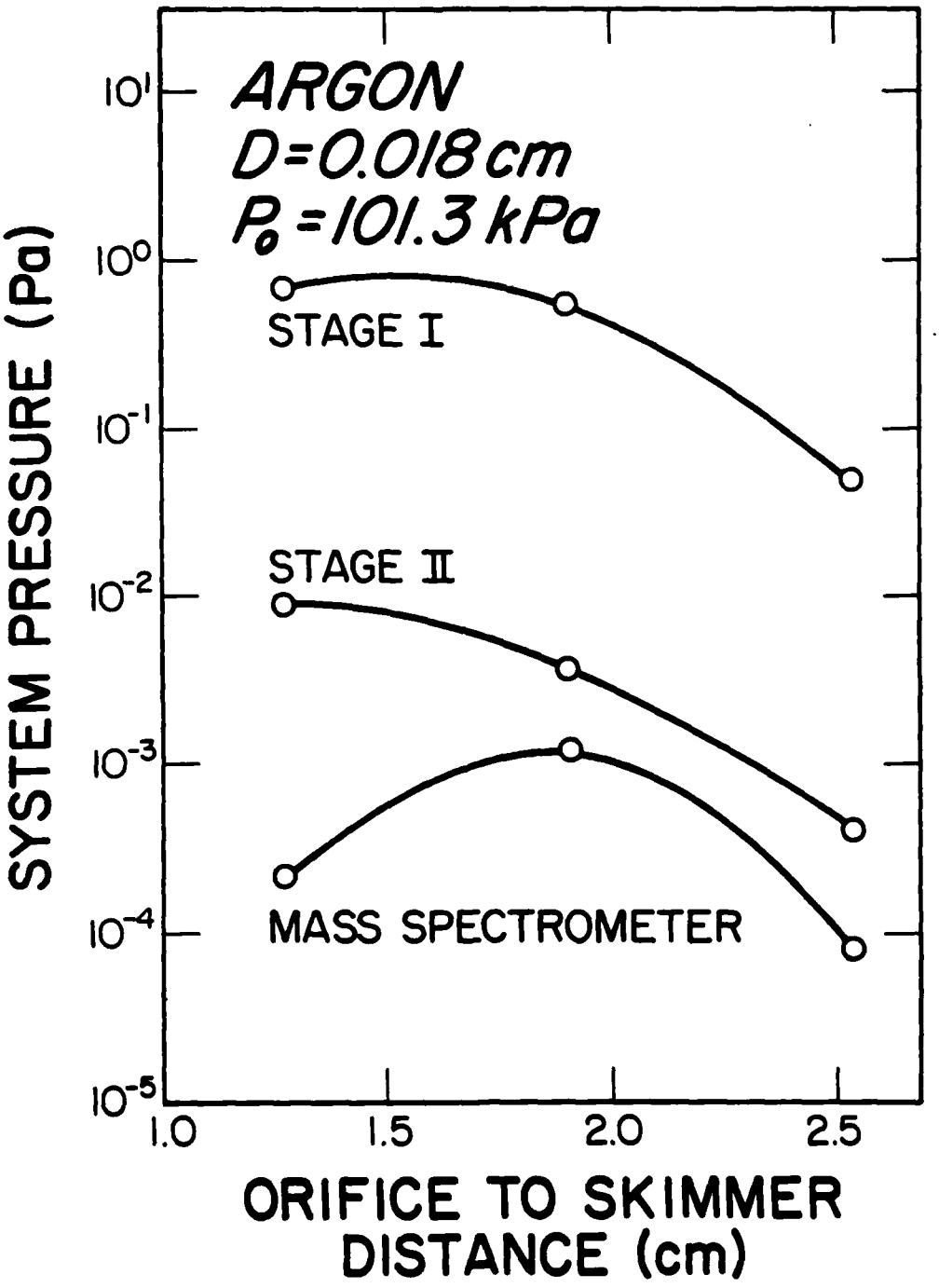
ARGON
D=0.018 cm
P_o=101.3 kPa
STAGE I
STAGE II
MASS SPECTROMETER
SYSTEM PRESSURE (Pa)
10^1
10^0
10^{-1}
10^{-2}
10^{-3}
10^{-4}
10^{-5}
1.0
1.5
2.0
2.5
ORIFICE TO SKIMMER DISTANCE (cm)

FIG. 6

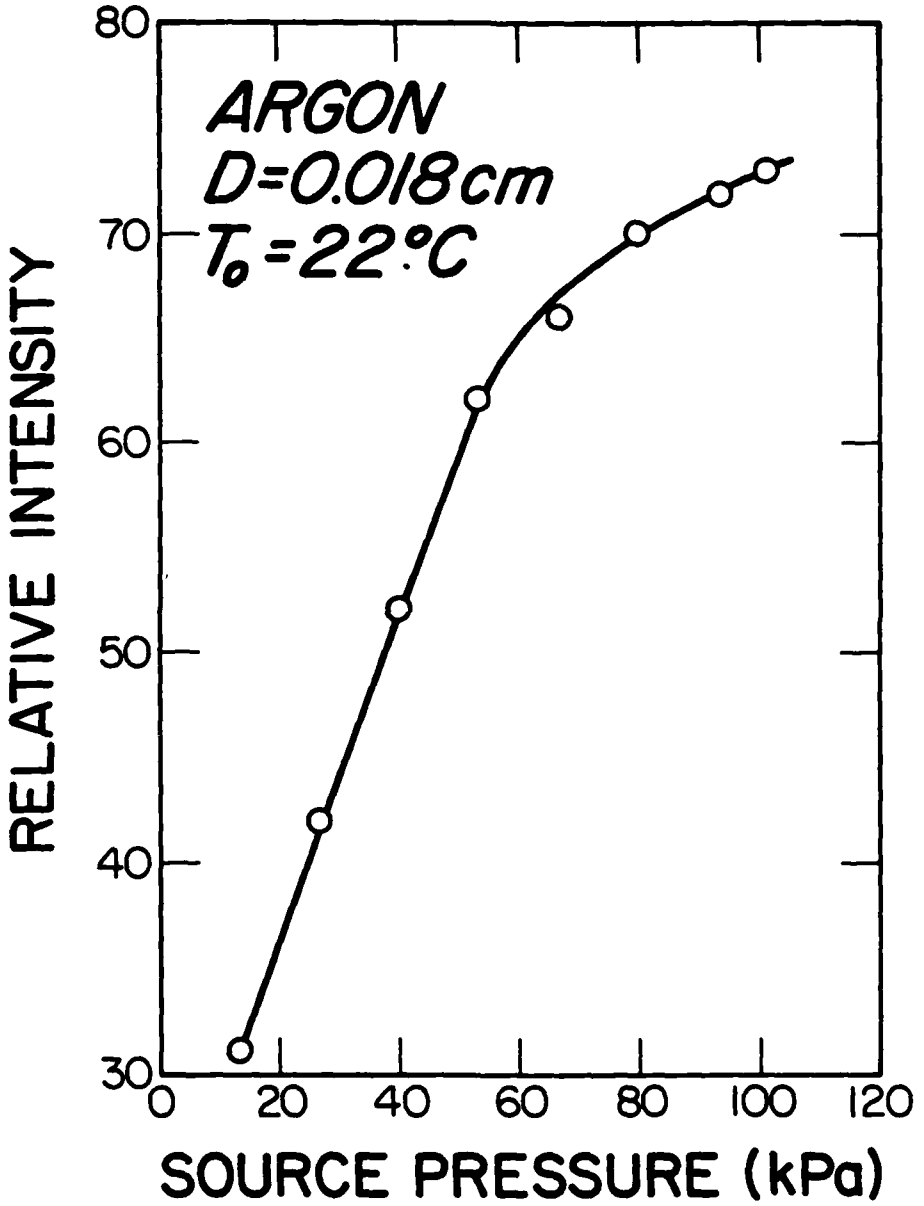
ARGON
D=0.018cm
T_o=22°C
RELATIVE INTENSITY
80
70
60
50
40
30
0
20
40
60
80
100
120
SOURCE PRESSURE (kPa)

FIG. 7

APPENDIX B

Equilibrium Calculations Using SOLGASMIX-PV

by

John E. Marra

and

Eric R. Kreidler

PROGRESS REPORT

EQUILIBRIUM CALCULATIONS USING SOLGASMIX-PV

INTRODUCTION:

The SOLGASMIX-PV program is proving to be most useful in studying the equilibrium relationships present in the systems under consideration. In accordance with the major thrust of this research, preliminary studies have been completed on nine distinct systems. These include SiC, Si_3N_4, and SiO_2 in HCl/Ar, HF/Ar, and H_2O/Ar atmospheres. The Si/HCl-Ar system has also been briefly studied.

After considerable time and effort, the program has been successfully debugged and is producing output in the expected format. Various changes have been made to correct the errors in the as-received program that resulted from slight system differences. These changes were made such that the operation of the program was not altered. Slight modifications have also been noted (by asterisks) in the program listing to allow data to be input as it appears in the JANAF[1] tables. (Since the program utilizes thermodynamic data in joules and the JANAF tables present such data in calories, program steps were added to accomodate this difference.)

As expected, the major problem encountered in the work conducted to date has been in the location of reliable thermodynamic data. Unfortunately even the most complete set of tables lacks data on numerous compounds of interest. The silicon-oxy-chloride compounds pose the greatest problem, as no pertinent data has been obtained for any of the compounds in this group. However in the interest of producing preliminary results,

the runs were performed using the most believable data that is currently available.

RESULTS AND DISCUSSION:

By means of the existing thermodynamic tables[1-5], a data base has been generated for use with the program. As stated before data was unobtainable for certain compounds, however, as more data becomes available it may easily be added to the data base and the necessary runs may be updated. The JANAF tables have been used as the main source for the data base in the preliminary work. While they are not the most current set of tables for a number of compounds, they are the most complete, consistent set of tables, and present data in a convenient form.

It should be noted that the program contains a provision for compounds with unknown data. However, the use of this provision is not fully understood, since any compounds entered without sufficient data are set equal to zero during the course of the calculations. The program most likely assigns a large free energy function value to the compounds with unknown data, making their likelihood of formation slim.

1. SiC-HCl System:

The preliminary work on this system involved 50 different species, that may be viewed as being candidates for formation in this system. Recently Fischman[6] has performed calculations on this system using the same SOLGAS program, which has provided a comparison standard for the present work. Although the majority of Fischman's work concentrated on systems with no Cl present, output given for systems containing both H and Cl provided

results in accordance with those generated here.

A typical set of data for this system is shown in Table I. Data is given for the equilibrium reaction between 10 moles of SiC and 4 moles of HCl at four different temperatures (1000, 1300, 1500, and 1700 ^{o}K). The program generates the partial pressure of each gaseous species (in a system with a total pressure of one atmosphere) and the molar quantity of each condensed species. The data shown was used to construct a plot of log partial pressure versus temperature for the $SiCl_x$ species.

Figure 1 compares the plot generated using data from the SOLGASMIX-PV program to a similar one obtained by simply analyzing the reaction:

$$SiC + x\ HCl = SiCl_x + x/2\ H_2 + C$$

Differences in these plots are obvious and are easily explained by the fact that the SOLGAS program considers all the species that may be present (in minimizing the free energy), and not just the ones taking part in the given reaction. The consideration of the numerous side reactions should produce more realistic results, however, proof of this statement will not be obtained until mass spectrometric analysis is completed.

Referring to the SOLGAS generated plot it is observed that $SiCl_4$ is predicted to be the most prevalent $SiCl_x$ species below ~1520 ^{o}K with $SiCl_3$ becoming dominant above this temperature. The graph obtained by considering merely the species specific to the given reaction predicts that $SiCl_3$ will be more prevalent than $SiCl_4$ throughout the temperature range tested. This plot also shows that $SiCl_2$ will become the most prevalent species

above 1660 ^{o}K, which is not observed in the computer generated plot.

Table I also illustrates several interesting properties of SiC during reaction with HCl. At all of the temperatures examined, all of the SiC is present in the form of β-SiC, which is expected. It is also interesting to note that approximately 10% of the SiC will be volatilized at the temperatures tested. This also is not too surprising. Since no oxygen is present, the protective SiO_2 layer (that acts as a corrosion inhibitor) does not form , and as a result a fairly violent reaction occurs. However, it is very surprising to note that the SiC appears to become more stable as the temperature increases. These results are opposite of those intuitively expected, but are consistent with the decrease in the amounts of the $SiCl_x$ compounds formed at the elevated temperatures. Comparing this data with that obtained through use of the mass spectrometer will provide an indication of the accuracy of the SOLGASMIX-PV results.

2. Si_3N_4-HCl System:

Thermodynamic data for this system was more difficult to locate, resulting in the consideration of only 31 species in the first set of calculations. Equilibrium data considering 2.5 moles of Si_3N_4 and 4 moles of HCl is summarized in Table II. As in the SiC system, a plot has been developed representing log partial pressure versus temperature for the $SiCl_x$ species (Fig. 2). Comparing Fig. 2 with Fig. 1, it is observed that the plots obtained using the data from the SOLGAS program are quite similar. The only major difference being that the $SiCl_2$ species

becomes more prevalent at the higher temperatures in the Si_3N_4 system.

The results listed in Table II also indicate that a number of gases should appear as relatively large peaks on a mass spectrometer trace. These gases include $SiCl_4$, $SiCl_3$, H_2, HCl, and N_2. This data represents compounds with a range of molecular weights and may prove to be useful during calibration of the system.

Although all of the Si_3N_4 appears in the alpha form in the generated results, it must be noted that this is merely because thermodynamic data was unavailable for the beta form. The data generated also indicates that ~8% of the sample will be volatilized during the equilibrium reaction. However, contrary to the SiC case, more of the sample is volatilized at the higher temperatures (which is to be expected).

3. SiO_2-HCl System:

For the runs to date, 36 species have been considered in this system. Unfortunately, as mentioned before, the silicon oxy chlorides were omitted due to the lack of thermodynamic data. These compounds are expected to form during the course of the equilibrium reaction between SiO_2 and HCl, making their omission a serious shortcoming of these calculations. However, for the purpose of obtaining preliminary results these compounds were ignored.

The resulting data for this system is illustrated in Table III and plotted (as log partial pressure versus temperature) in Fig. 3. From these results it is observable that SiO_2 does not

react as completely with HCl as does SiC or Si_3N_4. The partial pressure of HCl in all cases is very nearly 1.0 atmosphere, verifying this observation. The only other gaseous species present in meaningful quantities are H_2, H_2O, and Cl (resulting from the dissosciation of HCl).

In contrast to the results previously reported, $SiCl_4$ is the predominant $SiCl_x$ species formed at all the temperatures studied. It should also be noted that the $SiCl_4$ is present at significantly lower partial pressures than in the SiC and Si_3N_4 systems. As further proof of the lack of reaction in this system, the data predicts that no SiO_2 will be consumed during the equilibrium reaction with HCl.

4. SiC-HF System:

Thermodynamic data was obtained for 51 species that may possibly be formed during the equilibrium reaction in this system. A compilation of partial pressure data for the system containing 10 moles of SiC and 4 moles of HF is given in Table IV. Using this data a log partial pressure versus temperature plot has been constructed for the SiF_x species, and is shown in Fig. 4.

By referring to Fig. 4 it is obvious that the SiF_4 species dominates at all the temperatures examined. The data generated using the SOLGASMIX-PV program predicts that relatively large amounts of H_2 and HF gases will be observed in this system, indicating an amount of HF in excess of that necessary to complete the reaction. It is also observed that as the temperature increases, the amount of carbon present also

increases. This may be attributed to the fact that as the amount of SiF_x (due to the volatilization of Si) increases, there is a greater depletion of Si in the SiC sample, thus causing it to become carbon-rich.

5. Si_3N_4-HF System:

Studies in this system included 36 species, of which 3 were condensed. The results obtained for this system considering 2.5 moles of Si_3N_4 and 4 moles of HF are summarized in Table V. As before, a plot of log partial pressure versus temperature was constructed for the SiF_x species. As was the case in the SiC system, the SiF_4 species was the dominant species at all of the temperatures examined.

As in the case of Si_3N_4 in HCl, it is interesting to note that there appears to be a number of gaseous species in this system that should be detectable by means of the mass spectrometer. The species present in the largest amounts are H_2, N_2, SiF_3, and SiF_4 and also may possibly be used as reference peaks for calibration of the mass spectrometer.

The reactions taking place in this system also appear to be more violent than in the other systems examined. The results generated using the SOLGAS program indicate that nearly one-half of a mole (~20%) of Si_3N_4 will be consumed in this reaction.

6. SiO_2-HF System:

The JANAF tables provide data on 5 condensed and 32 gaseous species that could possibly be formed during this reaction. Contrary to the SiO_2-HCl system, data was obtained for the $SiOX_2$ compound. However, this data is still somewhat suspect since the

heat of formation was calculated by comparison to related compounds.

The compiled results for the system of 5 moles of SiO_2 reacting with 4 moles of HF are given in Table VI. As expected, a relatively large amount of SiO_2 (~1/2 mole) was consumed during this reaction. It appears that the majority of the Si volatilized goes into the formation of SiF_4. A plot of log partial pressure versus temperature for this system (Fig. 6) shows that SiF_4 is indeed the most predominant species.

7. SiC-H_2O System:

Preliminary studies in this system included 8 condensed and 40 gaseous species. Data for this system with 10 moles of SiC and 4 moles of H_2O is given in Table VII. It is obvious from the results presented in this table that the major gaseous product is H_2. The SOLGAS results also predict that relatively large quantitites of CO, H_2O, and SiO will also be observed when the system is examined using the mass spectrometer.

The data obtained for the condensed species in this system is interesting and appears to give the expected results. On the average two moles of SiC are consumed during the reaction. The Si that has been volatilized combines with the oxygen that is present (from the H_2O) to form the protective SiO_2 layer that has been confirmed to exist. It is important to note that at temperatures below 1700 kelvin the results predict that a carbon-rich layer will form between the SiC and the SiO_2 as a result of Si-depletion. At temperatures greater than 1700 ^oK, the carbon will also volatilize to form various carbon containing gases

(predominantly CO).

These predictions may be verified by analyzing the sample following testing in the flow reactor. By analyzing a cross-section of the sample using the scanning electron microscope, the presence of a protective SiO_2 layer and a carbon-rich interface may be detected. Analysis by EDS and Auger sputtering techniques may also prove useful in identification and characterization of the surface coatings.

8. Si_3N_4-H_2O System:

The runs conducted on this system to date have considered 44 distinct species, of which 7 were condensed. Preliminary results for the equilibrium reaction between 2.5 moles of Si_3N_4 and 4 moles of H_2O are summarized in Table VIII. These results indicate that in this atmosphere, a major transition occurs in the silicon nitride sample.

According to the data generated, all of the Si_3N_4 will be transformed to SiO_2 (in the form of quartz or cristobalite) or silicon oxy nitride (Si_2N_2O). While the presence of Si_2N_2O has been verified in Si_3N_4 samples following oxidation, it is misleading to believe that a complete transformation will occur. The results generated by the SOLGAS program are confusing in this case and care must be taken to avoid misinterpretation.

The thermodynamic data entered for this run indicates that the likelihood of formation of Si_2N_2O is greater than that for Si_3N_4. This represents a problem in the future calculations, particularly in the input amount of each material. The SOLGAS

input guide calls for data to be entered as elemental amounts and not simply the molar quantity of each compound. In other words, data for Si_3N_4 is entered as initial moles of Si(ref) and N_2 and not as moles of Si_3N_4. Thus when Si_2N_2O is considered in the calculations, it is formed preferentially to Si_3N_4 when the program combines the initial amounts of Si and N.

In reality a total transformation would not be expected to occur. After heating Si_3N_4 in an oxygen-containing atmosphere, a Si_2N_2O surface layer would most likely be formed, while the interior of the sample would remain as silicon nitride. Again, this prediction may easily be confirmed following mass spectrometric analysis.

The effect of oxygen content on this system was also briefly examined. The initial amount of water present was decreased and the final amounts of the condensed species formed were analyzed. The results obtained for this analysis at 1000 ^{o}K are presented in Table IX.

For the reasons discussed previously, all of the oxygen present goes into the formation of the silicon oxy nitride. Thus, decreasing the amount of oxygen present while maintaining a constant amount of Si and N would be expected to result in an increase in the amount of Si_3N_4 and a decrease in the amount of Si_2N_2O formed.

The results generated by the SOLGAS program confirm this statement. When only 3 moles of H_2O are present, 3 moles of silicon oxy nitride are formed, indicating that the amount of oxygen is limiting the extent of the formation reaction. Similar results are also observed when the amount of water is further

decreased.

9. SiO_2-H_2O System:

The equilibrium composition for this system was calculated using thermodynamic data on 22 separate compounds. The output generated by the SOLGASMIX-PV program is presented in Table X. The results given represent the equilibrium reaction between 5 moles of SiO_2 and 4 moles of H_2O.

It is obvious from the data shown that little or no reaction occurs when SiO_2 is heated in the presence of H_2O. There is no change in the number of moles of the silica sample. Further proof of the inert behavior of SiO_2 in this environment is given by the fact that nearly all of the gas present is in the form of water vapor. The only other gases present in meaningful quantities are H_2 and O_2, which result from the dissosciation of H_2O.

10. Si-HCl System:

The equilibrium between Si and HCl is of great importance to the semiconductor industry. Many materials from this system have been used as starting materials in the production of high-grade silicon, and as a result much research has been conducted regarding the thermodynamics of this system.

The data available has been used to compare the results generated by the SOLGASMIX-PV program to those obtained through the use of the Gordon-McBride[7] free energy minimization program. Herrick and Sanchez-Martinez[8] have recently used a modified version of the Gordon-McBride program to study this system at various temperatures.

various temperatures.

To obtain a "quick" comparison, the SOLGAS program was run under conditions similar to one of the runs reported by Herrick. The data for equilibrium at 1600 ^{o}K with a Cl/H ratio of 0.1 is summarized in Table XI. Brief examination of this table proves that the SOLGAS results are comparable to those obtained by Herrick for many of the species considered. The slight discrepancies that are observed may be explained by the fact that slightly different values of the heats of formation were used for these compounds.

The differing values used by Herrick appear to be from tables[9,10] that are more current than those given in the JANAF tables (which were used in the SOLGAS calculations). These values may prove useful when the data base is updated and the corresponding runs are repeated.

CONCLUSIONS:

The study of complex chemical equilibria requires the use of a powerful computer program. The SOLGASMIX-PV program is capable of performing such calculations for complex, multiphase systems. The program easily generates accurate equilibrium data for systems that have not been previously studied, providing that reliable thermodynamic input data is available for the compounds under consideration.

The data generated to date has proven to be most informative. By reviewing the results, "clues" on what to look for when using mass spectrometric analysis are easily obtained. In particular the program predicts that:

1. SiC and Si_3N_4 will react relatively violently in the

presence of HCl and HF.

2. Silica is fairly inert in HCl, but reacts vigorously in the presence of HF gas.
3. A protective SiO_2 layer will be formed on SiC in an H_2O atmosphere. A carbon-rich layer may also be observed, depending on the temperature at which the analysis is run.
4. Si_2N_2O will form on Si_3N_4 in the presence of H_2O.
5. The presence of H_2O has very little effect on the behavior of SiO_2 at temperatures between 1000 and 1700 ^oK.

The accuracy of the SOLGASMIX-PV program has also been tested by comparing output generated for the Si-HCl system (at 1600 ^oK) to published data. Results from the SOLGAS program agree extremely well with the published values, which were obtained using the Gordon-McBride free energy program.

The results generated in the preliminary studies indicate that further study of complex chemical equilibria, using the free energy minimization technique, is warranted. Since information is generated so rapidly (at relatively little expense), systems that have not been previously studied may easily be examined. Previous knowledge of the species present in a system is not absolutely necessary.

RECOMMENDATIONS FOR FUTURE WORK:

In accordance with the problems encountered in the preliminary work, a search should be conducted in order to locate more current, and previously unavailable, thermodynamic data. The availability of the CAS online service and other similiar services at the University present the perfect opportunity for such a search.

Since the preliminary results also indicate that data obtained may possibly be used in calibration of the mass spectrometer, further study should be undertaken in this area. When experimental work is begun, the conditions of each run should be accurately recorded. This data may in turn be entered into the SOLGAS program to generate theoretical data for a given system. This data will not only give the experimenter an idea of the species that will be present, but will also indicate what species will be present in the largest amounts. These species may be used as reference peaks in a mass spectrometer trace.

The complexity of many species has previously made the study of chemical equilibria impractical. The SOLGAS program has proven that it can easily handle even the most complex systems. Although the program has been available for several years, it has not been effectively used. Future work should also include the generation of equilibrium data for systems of importance which have not been previously studied. The publication of these results may prove useful to other researchers.

APPENDIX

TABLES AND FIGURES

[Note: Species present at partial pressures less than 10^{-20} atm are assumed to be undetectable and are set equal to zero in the following tables.]

TABLE I

Typical output for the SiC-HCl System.

Species	Partial Pressure (atm) 1000 °K	1300 °K	1500 °K	1700 °K
C(g)	0	0	1.9×10^{-17}	1.7×10^{-14}
CCl	0	1.1×10^{-19}	2.8×10^{-16}	0
CCl_2	0	3.2×10^{-17}	1.7×10^{-14}	1.6×10^{-12}
CCl_3	0	2.3×10^{-19}	8.9×10^{-17}	6.1×10^{-15}
CCl_4	0	0	2.5×10^{-19}	1.1×10^{-17}
CH	0	6.5×10^{-19}	8.5×10^{-16}	2.0×10^{-13}
CHCl	0	3.3×10^{-16}	9.4×10^{-14}	6.2×10^{-12}
$CHCl_3$	9.5×10^{-20}	6.1×10^{-16}	2.1×10^{-14}	2.3×10^{-13}
CH_2	6.0×10^{-19}	1.8×10^{-14}	1.6×10^{-12}	4.6×10^{-11}
CH_2Cl_2	2.6×10^{-13}	3.0×10^{-11}	1.8×10^{-10}	5.5×10^{-10}
CH_3	1.9×10^{-9}	5.8×10^{-8}	2.1×10^{-7}	5.7×10^{-7}
CH_3Cl	1.9×10^{-7}	4.4×10^{-7}	4.6×10^{-7}	4.2×10^{-7}
$SiCH_3Cl_3$	2.4×10^{-6}	6.0×10^{-7}	2.0×10^{-7}	4.5×10^{-13}
CH_4	3.0×10^{-2}	1.5×10^{-3}	3.0×10^{-4}	8.4×10^{-5}
SiC(g)	0	0	6.3×10^{-18}	1.1×10^{-14}
Si_2C	0	3.1×10^{-17}	1.2×10^{-13}	6.0×10^{-11}
C_2	0	0	9.0×10^{-20}	2.4×10^{-16}
C_2Cl_2	0	8.6×10^{-16}	3.2×10^{-13}	2.4×10^{-11}
C_2Cl_4	0	0	0	9.2×10^{-19}
C_2Cl_6	0	0	0	0
C_2H	6.1×10^{-19}	2.8×10^{-13}	8.3×10^{-11}	6.3×10^{-9}
C_2HCl	2.7×10^{-15}	4.6×10^{-11}	2.9×10^{-9}	6.1×10^{-8}
C_2H_2	7.7×10^{-10}	3.0×10^{-7}	3.6×10^{-6}	2.4×10^{-5}
C_2H_4	1.9×10^{-7}	3.3×10^{-7}	3.1×10^{-7}	3.0×10^{-7}

TABLE I (CONT.)

SiC_2	0	3.0×10^{-17}	1.3×10^{-13}	7.8×10^{-11}
C_3	0	0	4.7×10^{-18}	7.8×10^{-11}
C_4	0	0	0	1.0×10^{-19}
C_5	0	0	0	1.6×10^{-19}
Cl	2.9×10^{-10}	4.6×10^{-7}	1.1×10^{-5}	1.1×10^{-4}
HCl	9.8×10^{-2}	3.2×10^{-1}	4.5×10^{-1}	5.2×10^{-1}
SiH_3Cl	1.2×10^{-4}	9.9×10^{-5}	6.7×10^{-5}	4.5×10^{-5}
SiCl	9.1×10^{-15}	6.1×10^{-10}	7.5×10^{-8}	2.6×10^{-6}
Cl_2	5.1×10^{-13}	1.3×10^{-9}	3.5×10^{-8}	3.4×10^{-7}
SiH_2Cl_2	5.2×10^{-4}	6.4×10^{-4}	4.9×10^{-4}	3.3×10^{-4}
$SiCl_2$	7.5×10^{-6}	1.3×10^{-3}	1.1×10^{-2}	4.1×10^{-2}
$SiHCl_3$	3.5×10^{-2}	2.7×10^{-2}	1.7×10^{-2}	8.8×10^{-3}
$SiCl_3$	2.1×10^{-3}	3.0×10^{-2}	7.1×10^{-2}	9.8×10^{-2}
$SiCl_4$	2.9×10^{-1}	1.8×10^{-1}	1.0×10^{-1}	4.3×10^{-2}
H_2	5.5×10^{-1}	4.4×10^{-1}	3.4×10^{-1}	2.8×10^{-1}
SiH_4	7.4×10^{-11}	6.0×10^{-10}	1.2×10^{-9}	1.9×10^{-9}
Si(g)	6.3×10^{-20}	1.2×10^{-13}	7.2×10^{-11}	9.5×10^{-9}
Si_2	0	9.1×10^{-20}	7.0×10^{-16}	6.5×10^{-13}
Si_3	0	0	9.2×10^{-19}	2.4×10^{-15}
H	1.7×10^{-9}	7.3×10^{-7}	1.0×10^{-5}	7.8×10^{-5}
Ar	0	0	0	0
Values listed below are molar quantities.				
Si(l)	0	0	0	0
Si(ref)	0	0	0	0
α-SiC	0	0	0	0
β-SiC	9.04	9.21	9.29	9.30
C(graph)	0.87	0.79	0.71	0.70

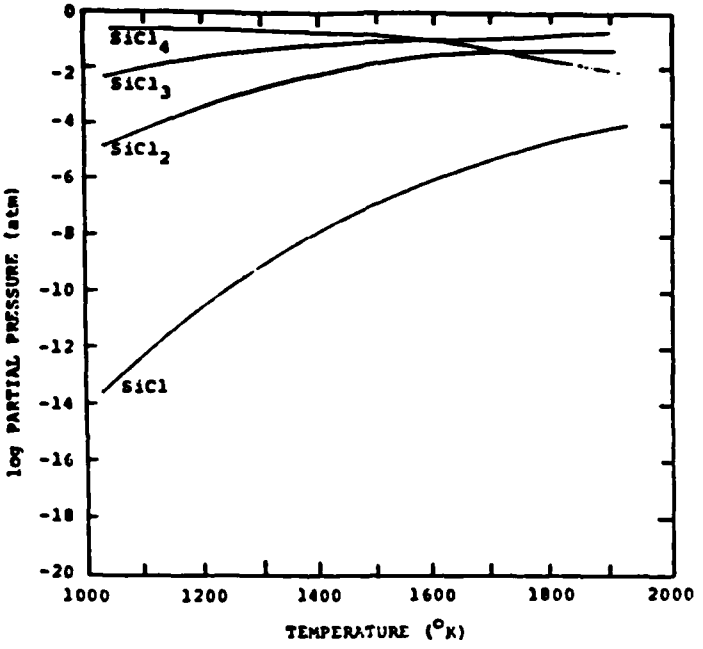

a. SOLGASMIX-PV generated plot.

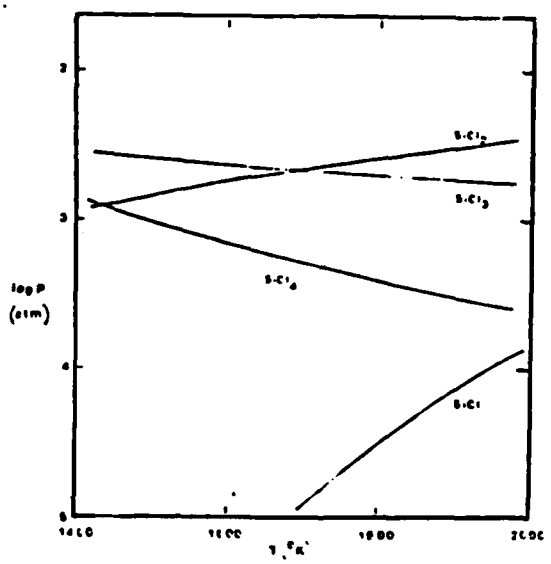

b. Plot obtained by considering the reaction:
$SiC + x\ HCl = SiCl_x + x/2\ H_2 + C$

Fig. 1. Log partial pressure versus temperature plots for the $SiCl_x$ species in the SiC-HCl system.

TABLE II

Typical output for the Si_3N_4-HCl system.

Species	Partial Pressure (atm) 1000 °K	1300 °K	1500 °K	1700 °K
$SiHCl_3$	2.9×10^{-3}	1.0×10^{-2}	1.3×10^{-2}	1.7×10^{-3}
SiH_2Cl_2	6.2×10^{-6}	1.2×10^{-4}	3.5×10^{-4}	5.4×10^{-4}
SiH_3Cl	2.1×10^{-6}	8.9×10^{-6}	4.1×10^{-5}	1.1×10^{-4}
SiCl	3.4×10^{-17}	9.7×10^{-11}	5.9×10^{-8}	6.0×10^{-6}
$SiCl_2$	1.5×10^{-7}	3.5×10^{-4}	8.6×10^{-3}	6.4×10^{-2}
$SiCl_4$	1.6×10^{-1}	1.4×10^{-1}	9.0×10^{-2}	3.1×10^{-2}
SiH_4	1.9×10^{-14}	2.7×10^{-11}	6.3×10^{-10}	6.7×10^{-9}
Si(g)	4.5×10^{-23}	1.1×10^{-13}	5.4×10^{-11}	3.2×10^{-8}
Si_2	0	0	4.0×10^{-16}	7.2×10^{-12}
Si_3	0	0	4.0×10^{-19}	9.0×10^{-14}
Ar	0	0	0	0
NH_3	3.7×10^{-5}	6.7×10^{-6}	3.3×10^{-6}	2.2×10^{-6}
N_2H_4	3.2×10^{-19}	2.8×10^{-18}	8.2×10^{-18}	2.4×10^{-17}
$SiCl_3$	2.3×10^{-4}	1.3×10^{-2}	5.9×10^{-2}	1.0×10^{-1}
N_2H_2	4.4×10^{-19}	1.2×10^{-16}	1.6×10^{-15}	1.4×10^{-14}
Cl_2	1.4×10^{-11}	3.6×10^{-9}	3.7×10^{-8}	1.6×10^{-7}
H_2	3.3×10^{-1}	3.0×10^{-1}	2.9×10^{-1}	2.9×10^{-1}
Cl	1.5×10^{-9}	7.6×10^{-7}	1.1×10^{-5}	7.8×10^{-5}
H	1.3×10^{-9}	6.0×10^{-7}	9.5×10^{-6}	7.9×10^{-5}
HCl	3.9×10^{-1}	4.3×10^{-1}	4.2×10^{-1}	3.6×10^{-1}
N_2	1.1×10^{-1}	1.1×10^{-1}	1.1×10^{-1}	1.4×10^{-1}
NH	4.2×10^{-18}	4.8×10^{-14}	3.2×10^{-12}	8.6×10^{-11}
SiH	0	5.5×10^{-14}	1.0×10^{-10}	2.8×10^{-8}
N	0	5.3×10^{-17}	2.0×10^{-14}	2.0×10^{-12}

TABLE II (CONT.)

SiN	0	1.3×10^{-14}	2.5×10^{-11}	7.6×10^{-9}
Si_2N	0	4.5×10^{-18}	2.2×10^{-13}	7.2×10^{-10}
H_2N	9.2×10^{-12}	2.0×10^{-10}	1.5×10^{-9}	7.4×10^{-9}
Values listed below are molar quantities.				
NH_4Cl	0	0	0	0
Si(ref)	0	0	0	0
Si(liq)	0	0	0	0
α-Si_3N_4	2.29	2.30	2.28	2.21

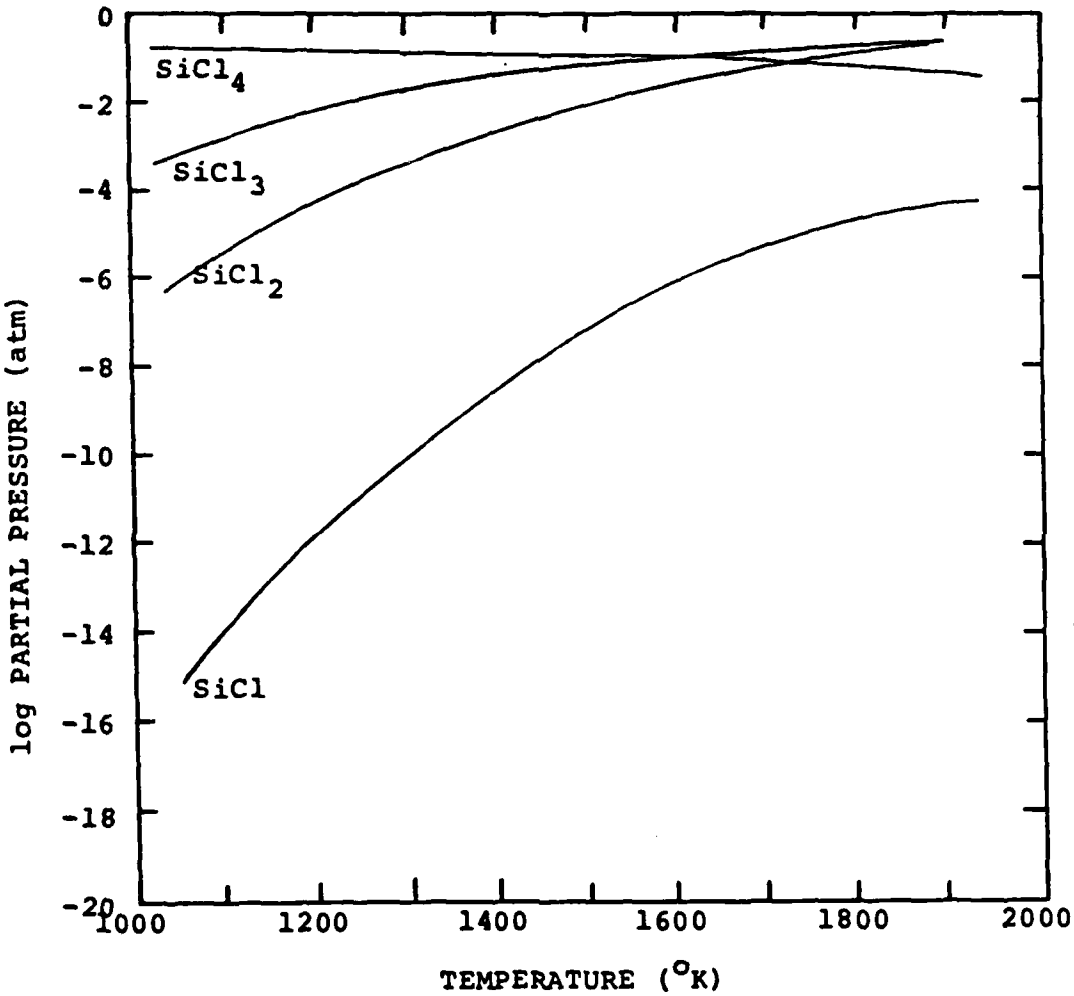

Fig. 2. Log partial pressure versus temperature plot for the $SiCl_x$ species in the Si_3N_4-HCl system.

TABLE III

Typical output for the SiO_2-HCl system.

Species	Partial Pressure (atm) 1000 °K	1300 °K	1500 °K	1700 °K
Cl	9.1×10^{-7}	9.6×10^{-5}	6.7×10^{-4}	2.9×10^{-3}
HCl	1.0	1.0	1.0	9.9×10^{-1}
HClO	3.5×10^{-12}	6.2×10^{-10}	5.0×10^{-9}	2.3×10^{-8}
H_3SiCl	0	0	0	0
ClO	1.4×10^{-16}	1.4×10^{-12}	6.3×10^{-11}	9.8×10^{-10}
ClO_2	0	0	3.0×10^{-20}	2.2×10^{-18}
SiCl	0	1.1×10^{-19}	1.5×10^{-15}	2.5×10^{-12}
Cl_2	5.2×10^{-6}	5.5×10^{-5}	1.3×10^{-4}	2.2×10^{-4}
SiH_2Cl_2	1.5×10^{-19}	5.3×10^{-15}	8.2×10^{-13}	4.6×10^{-11}
Cl_2O	0	8.3×10^{-18}	4.8×10^{-16}	8.8×10^{-15}
$SiCl_2$	2.1×10^{-16}	4.7×10^{-11}	1.3×10^{-8}	9.9×10^{-7}
$HSiCl_3$	1.2×10^{-19}	1.5×10^{-15}	8.6×10^{-14}	1.7×10^{-12}
$SiCl_3$	2.0×10^{-10}	2.2×10^{-7}	5.2×10^{-6}	5.9×10^{-5}
$SiCl_4$	8.3×10^{-5}	2.8×10^{-4}	4.7×10^{-4}	6.6×10^{-4}
H	5.4×10^{-12}	1.1×10^{-8}	3.8×10^{-7}	5.9×10^{-6}
OH	3.4×10^{-13}	7.8×10^{-10}	2.2×10^{-8}	2.7×10^{-7}
HO_2	0	1.1×10^{-18}	2.0×10^{-16}	9.2×10^{-15}
SiH	0	0	0	2.4×10^{-17}
H_2	5.7×10^{-6}	1.0×10^{-4}	4.6×10^{-4}	1.6×10^{-3}
H_2O	1.7×10^{-3}	5.6×10^{-4}	9.4×10^{-4}	1.4×10^{-3}
H_2O_2	0	1.4×10^{-17}	7.6×10^{-16}	6.2×10^{-13}
SiH_4	0	0	0	0
O	4.0×10^{-19}	8.2×10^{-14}	1.6×10^{-11}	7.9×10^{-10}
SiO	2.0×10^{-20}	4.1×10^{-13}	8.5×10^{-10}	3.1×10^{-7}

TABLE III (CONT.)

O_2	6.5×10^{-18}	2.2×10^{-13}	1.5×10^{-11}	3.8×10^{-10}
SiO_2	0	1.2×10^{-15}	1.8×10^{-12}	4.6×10^{-10}
O_3	0	0	0	0
Si(g)	0	0	2.4×10^{-20}	3.4×10^{-16}
Si_2	0	0	0	0
Si_3	0	0	0	0
Ar	0	0	0	0
Values listed below are molar quantities.				
Si(liq)	0	0	0	0
Si(ref)	0	0	0	0
SiO_2(liq)	0	0	0	0
SiO_2(cr)	0	5.00	5.00	5.00
SiO_2(q)	5.00	0	0	0

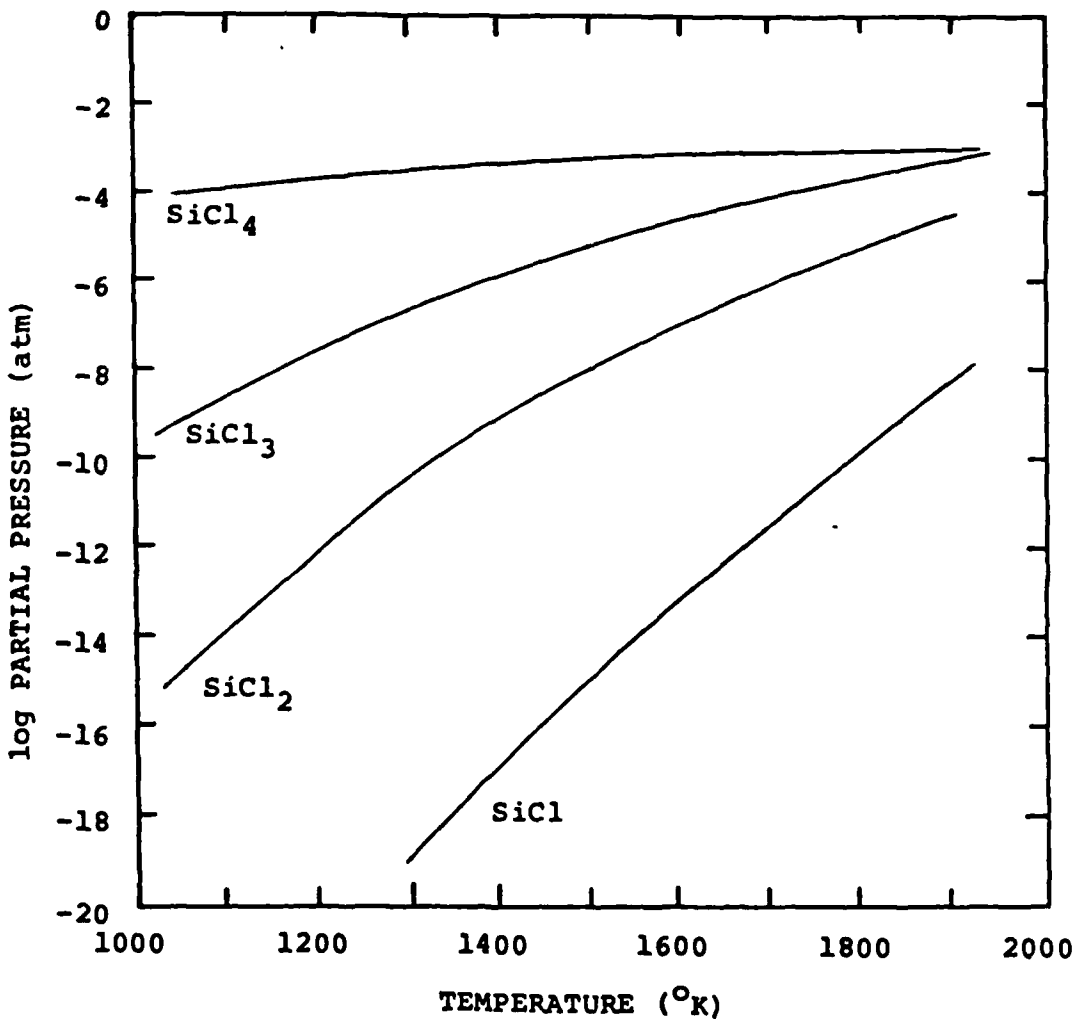

Fig. 3. Log partial pressure versus temperature plot for the $SiCl_x$ species in the SiO_2-HCl system.

TABLE IV

Typical output for the SiC-HF system.

Species	Partial Pressure (atm) 1000 °K	1300 °K	1500 °K	1700 °K
CF	0	2.9×10^{-19}	7.5×10^{-16}	2.9×10^{-13}
CF_2	0	1.8×10^{-19}	2.3×10^{-16}	5.1×10^{-14}
CF_3	0	0	0	2.2×10^{-19}
CF_4	0	0	0	0
CH	0	8.0×10^{-19}	1.2×10^{-15}	3.0×10^{-13}
CHF	0	2.8×10^{-17}	1.4×10^{-14}	1.5×10^{-12}
CHF_3	0	0	2.5×10^{-18}	1.5×10^{-16}
CH_2	6.8×10^{-19}	2.8×10^{-14}	3.0×10^{-12}	1.0×10^{-10}
CH_2F_2	1.1×10^{-19}	6.1×10^{-16}	2.6×10^{-14}	4.2×10^{-13}
CH_3	2.2×10^{-9}	1.1×10^{-7}	5.6×10^{-7}	1.9×10^{-6}
CH_3F	4.1×10^{-12}	2.0×10^{-10}	1.0×10^{-9}	3.4×10^{-9}
$SiCH_3F_3$	5.9×10^{-7}	4.5×10^{-7}	3.7×10^{-7}	0
CH_4	3.7×10^{-2}	3.4×10^{-3}	1.1×10^{-3}	4.2×10^{-4}
SiC(g)	0	0	6.3×10^{-18}	1.1×10^{-14}
Si_2C	0	0	1.9×10^{-17}	1.7×10^{-14}
C_2	0	0	1.8×10^{-19}	4.3×10^{-16}
C_2F_2	0	0	0	4.5×10^{-20}
C_2F_4	0	0	0	0
C_2F_6	0	0	0	0
C_2H	6.4×10^{-19}	3.4×10^{-13}	1.1×10^{-10}	9.5×10^{-9}
C_2HF	0	7.3×10^{-17}	3.8×10^{-14}	4.3×10^{-12}
C_2H_2	8.6×10^{-10}	4.5×10^{-7}	6.8×10^{-6}	5.3×10^{-5}
C_2H_4	2.3×10^{-7}	7.4×10^{-7}	1.1×10^{-6}	1.5×10^{-6}
SiC_2	0	3.0×10^{-17}	1.3×10^{-13}	7.8×10^{-11}

TABLE IV (CONT.)

C_3	0	0	4.7×10^{-18}	9.0×10^{-15}
C_4	0	0	0	1.9×10^{-19}
SiC_4H_{12}	2.0×10^{-16}	3.0×10^{-19}	4.9×10^{-21}	9.2×10^{-4}
C_5	0	0	0	1.6×10^{-19}
Ar	0	0	0	0
F	3.5×10^{-20}	1.5×10^{-14}	4.7×10^{-12}	3.7×10^{-10}
HF	9.3×10^{-5}	2.0×10^{-3}	7.7×10^{-3}	2.0×10^{-2}
$SiFH_3$	1.4×10^{-4}	2.0×10^{-4}	2.2×10^{-4}	2.2×10^{-4}
SiF	3.1×10^{-16}	5.2×10^{-11}	1.0×10^{-8}	5.7×10^{-7}
F_2	0	0	0	0
SiH_2F_2	3.5×10^{-4}	7.0×10^{-4}	8.8×10^{-4}	9.6×10^{-4}
SiF_2	1.0×10^{-8}	1.0×10^{-5}	2.1×10^{-4}	1.9×10^{-3}
$SiHF_3$	7.1×10^{-4}	2.2×10^{-3}	3.4×10^{-3}	4.2×10^{-3}
SiF_3	2.5×10^{-4}	8.2×10^{-3}	3.6×10^{-2}	9.9×10^{-2}
SiF_4	3.4×10^{-1}	3.3×10^{-1}	3.0×10^{-1}	2.4×10^{-1}
H	1.8×10^{-9}	8.9×10^{-7}	1.4×10^{-5}	1.2×10^{-4}
SiH	3.8×10^{-18}	8.6×10^{-13}	2.0×10^{-10}	1.2×10^{-8}
H_2	6.2×10^{-1}	6.6×10^{-1}	6.5×10^{-1}	6.3×10^{-1}
SiH_4	9.2×10^{-11}	1.4×10^{-9}	4.2×10^{-9}	9.4×10^{-9}
Si(g)	6.3×10^{-20}	1.2×10^{-13}	7.2×10^{-11}	9.5×10^{-9}
Si_2	0	9.1×10^{-20}	7.0×10^{-16}	6.5×10^{-13}
Si_3	0	0	9.3×10^{-19}	2.4×10^{-15}
Values listed below are molar quantities.				
Si(liq)	0	0	0	0
Si(ref)	0	0	0	0
β-SiC	9.0	9.0	9.0	8.9
α-SiC	0	0	0	0

TABLE IV (CONT.)

C(ref)	0.9	1.0	1.0	1.1

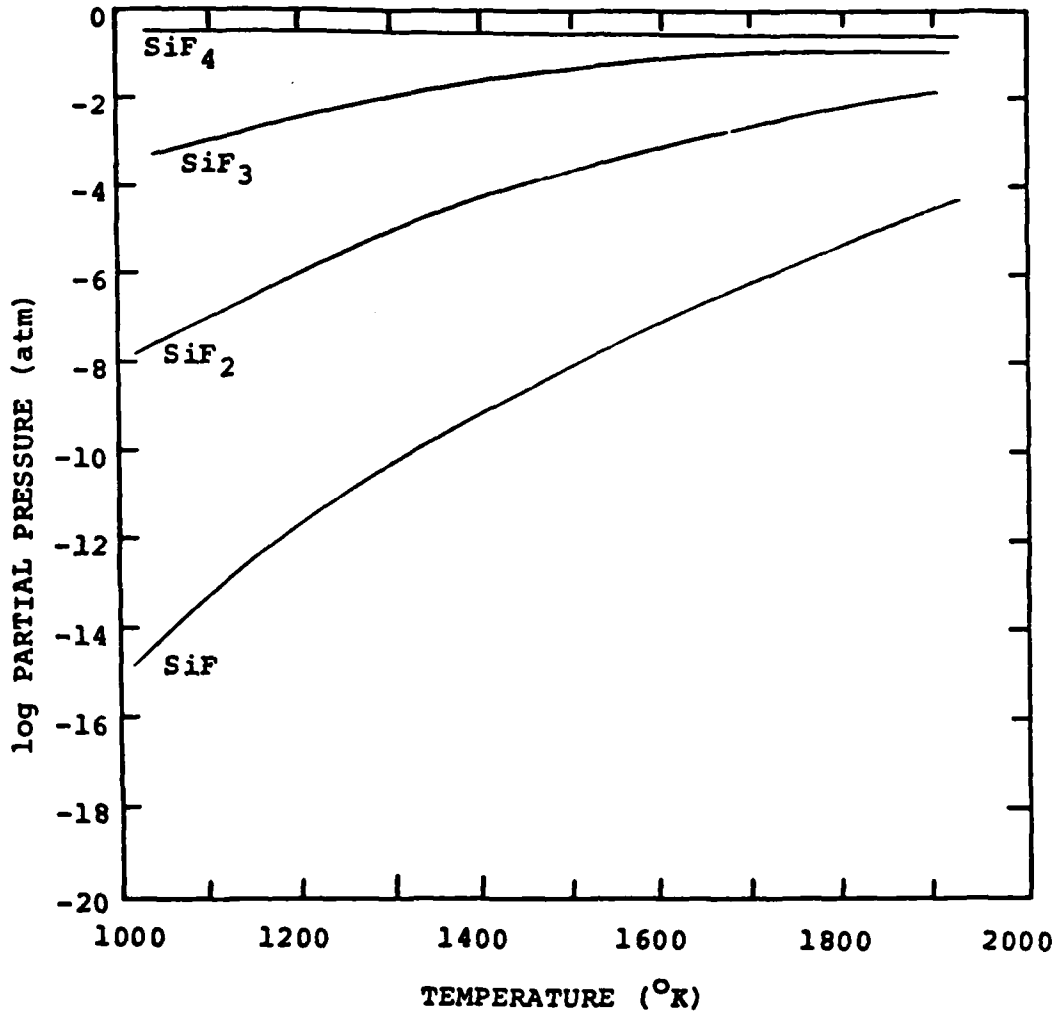

Fig. 4. Log partial pressure versus temperature plot for the SiF_x species in the SiC-HF system.

TABLE V

Typical output for the Si_3N_4-HF system.

Species	Partial Pressure (atm) 1000 °K	1300 °K	1500 °K	1700 °K
NF	0	0	1.7×10^{-20}	4.1×10^{-18}
NF_2	0	0	0	0
N_2F_2(C)	0	0	0	0
N_2F_2(T)	0	0	0	0
NF_3	0	0	0	0
N_2F_4	0	0	0	0
NH	7.0×10^{-18}	8.4×10^{-14}	5.4×10^{-12}	1.3×10^{-10}
NH_2	5.2×10^{-12}	4.7×10^{-10}	3.4×10^{-9}	1.5×10^{-8}
N_2H_2	1.2×10^{-18}	3.7×10^{-16}	4.6×10^{-15}	3.1×10^{-14}
NH_3	1.0×10^{-4}	2.1×10^{-5}	1.0×10^{-5}	5.7×10^{-6}
N_2H_4	1.1×10^{-18}	1.2×10^{-17}	3.5×10^{-17}	7.6×10^{-17}
N_2	1.8×10^{-1}	1.8×10^{-1}	1.8×10^{-1}	1.8×10^{-1}
Si_2N	0	2.7×10^{-18}	1.4×10^{-13}	5.4×10^{-10}
SiN	0	1.2×10^{-14}	2.3×10^{-11}	7.2×10^{-9}
N	6.1×10^{-6}	4.9×10^{-4}	3.4×10^{-3}	1.5×10^{-2}
F	2.2×10^{-19}	2.8×10^{-14}	5.2×10^{-12}	2.7×10^{-10}
HF	5.5×10^{-4}	3.5×10^{-3}	7.6×10^{-3}	1.3×10^{-2}
Ar	0	0	0	0
$SiFH_3$	3.8×10^{-7}	1.9×10^{-5}	1.0×10^{-4}	3.2×10^{-4}
SiF	1.0×10^{-18}	6.4×10^{-12}	6.4×10^{-9}	1.1×10^{-6}
F_2	0	0	0	0
SiH_2F_2	6.2×10^{-6}	1.3×10^{-4}	4.9×10^{-4}	1.1×10^{-3}
SiF_2	2.0×10^{-10}	2.4×10^{-6}	1.4×10^{-4}	2.7×10^{-3}
$SiHF_3$	8.4×10^{-5}	8.8×10^{-4}	2.3×10^{-3}	3.9×10^{-3}

TABLE V (CONT.)

SiF_3	3.2×10^{-5}	3.6×10^{-3}	2.7×10^{-2}	1.0×10^{-1}
SiF_4	2.7×10^{-1}	2.7×10^{-1}	2.5×10^{-1}	1.7×10^{-1}
H	1.7×10^{-9}	8.1×10^{-7}	1.3×10^{-5}	1.0×10^{-4}
SiH	1.8×10^{-20}	5.2×10^{-14}	1.0×10^{-10}	3.1×10^{-8}
H_2	5.5×10^{-1}	5.4×10^{-1}	5.3×10^{-1}	5.1×10^{-1}
SiH_4	3.7×10^{-14}	6.1×10^{-11}	1.6×10^{-9}	1.7×10^{-8}
Si(g)	0	7.8×10^{-15}	4.0×10^{-11}	2.7×10^{-8}
Si_2	0	0	2.2×10^{-16}	5.1×10^{-12}
Si_3	0	0	1.6×10^{-19}	5.4×10^{-14}
Values listed below are molar quantities.				
Si(liq)	0	0	0	0
Si(ref)	0	0	0	0
α-Si_3N_4	2.17	2.17	2.16	2.13

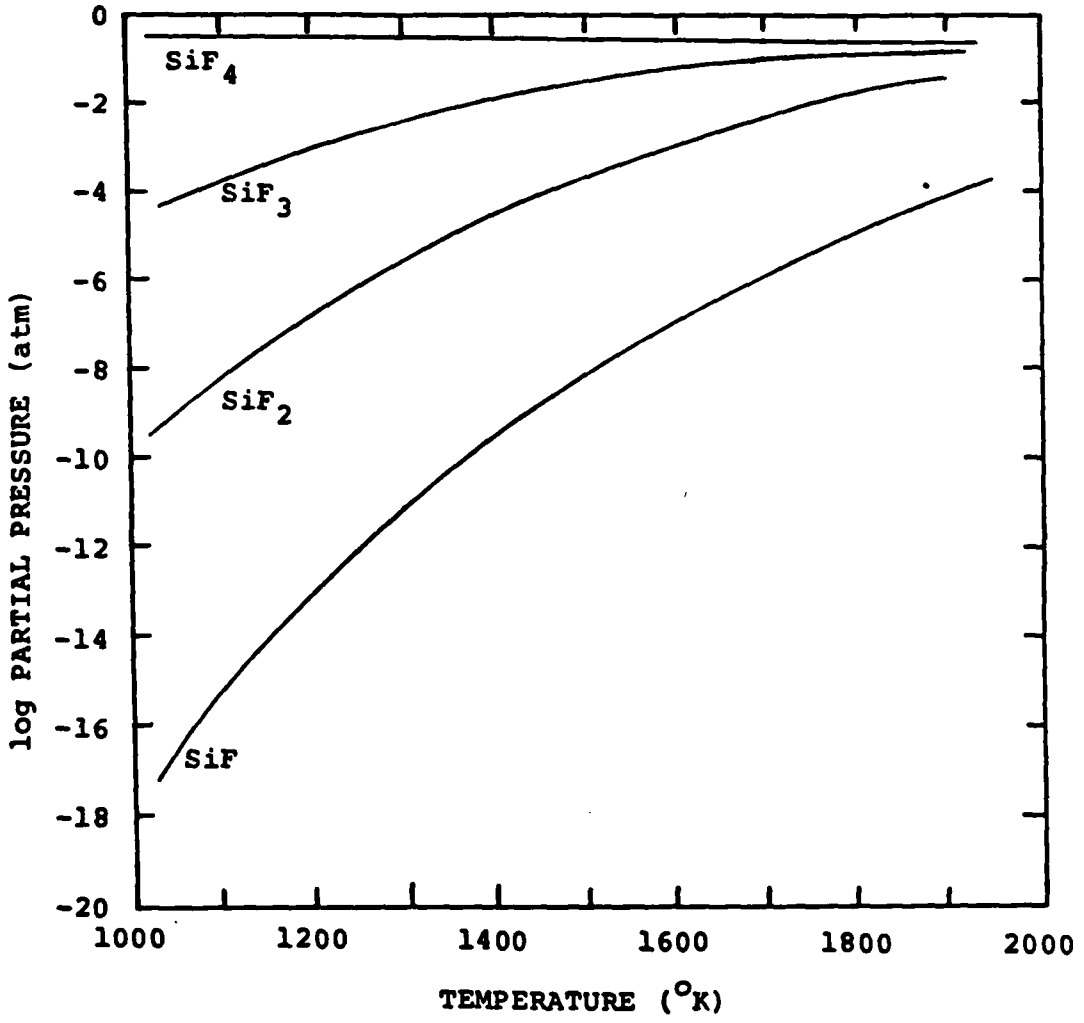

Fig. 5. Log partial pressure versus temperature plot for the SiF_x species in the Si_3N_4-HF system.

TABLE VI

Typical output for the SiO_2-HF system.

Species	Partial Pressure (atm) 1000 °K	1300 °K	1500 °K	1700 °K
OH	5.8×10^{-9}	1.3×10^{-6}	1.4×10^{-5}	7.7×10^{-5}
HFO	4.8×10^{-15}	3.4×10^{-12}	5.8×10^{-11}	4.5×10^{-10}
FO	0	4.5×10^{-16}	6.1×10^{-14}	2.5×10^{-12}
FO_2	0	5.7×10^{-18}	6.1×10^{-16}	2.0×10^{-14}
F_2O	0	0	0	1.7×10^{-20}
O_3	0	0	2.7×10^{-19}	2.0×10^{-17}
$SiOF_2$	5.0×10^{-11}	1.3×10^{-7}	3.8×10^{-6}	5.2×10^{-5}
HO_2	8.7×10^{-15}	9.5×10^{-12}	2.0×10^{-10}	1.8×10^{-9}
H_2O	4.5×10^{-1}	3.2×10^{-1}	2.5×10^{-1}	2.2×10^{-1}
H_2O_2	3.3×10^{-13}	4.0×10^{-11}	3.1×10^{-10}	4.2×10^{-7}
SiO_2(g)	0	1.4×10^{-15}	2.0×10^{-12}	5.1×10^{-10}
O_2	7.2×10^{-8}	5.5×10^{-6}	3.6×10^{-5}	1.4×10^{-4}
SiO	0	7.3×10^{-17}	5.0×10^{-13}	4.3×10^{-10}
O	4.2×10^{-14}	4.1×10^{-10}	2.4×10^{-8}	5.2×10^{-7}
F	2.5×10^{-13}	9.2×10^{-10}	3.5×10^{-8}	5.7×10^{-7}
HF	3.2×10^{-1}	5.3×10^{-1}	6.2×10^{-1}	6.6×10^{-1}
Ar	0	0	0	0
$SiFH_3$	0	0	0	3.0×10^{-19}
SiF	0	0	1.1×10^{-20}	7.4×10^{-17}
F_2	0	8.4×10^{-19}	1.6×10^{-16}	8.6×10^{-15}
SiH_2F_2	0	1.6×10^{-18}	8.0×10^{-16}	9.1×10^{-14}
SiF_2	0	1.3×10^{-15}	1.6×10^{-12}	3.8×10^{-10}
$SiHF_3$	3.2×10^{-14}	7.3×10^{-11}	2.1×10^{-9}	2.8×10^{-8}
SiF_3	2.3×10^{-11}	6.4×10^{-8}	2.0×10^{-6}	3.0×10^{-5}

TABLE VI (CONT.)

SiF_4	$2.3x10^{-1}$	$1.6x10^{-1}$	$1.3x10^{-1}$	$1.1x10^{-1}$
H	$8.6x10^{-13}$	$3.8x10^{-9}$	$1.5x10^{-7}$	$2.5x10^{-6}$
SiH	0	0	0	0
H_2	$1.5x10^{-7}$	$1.2x10^{-5}$	$7.8x10^{-5}$	$3.0x10^{-4}$
SiH_4	0	0	0	0
Si(g)	0	0	0	0
Si_2	0	0	0	0
Si_3	0	0	0	0
Values listed below are molar quantities.				
Si(liq)	0	0	0	0
Si(ref)	0	0	0	0
SiO_2(q)	4.26	0	0	0
SiO_2(cr)	0	4.45	4.56	4.60
SiO_2(liq)	0	0	0	0

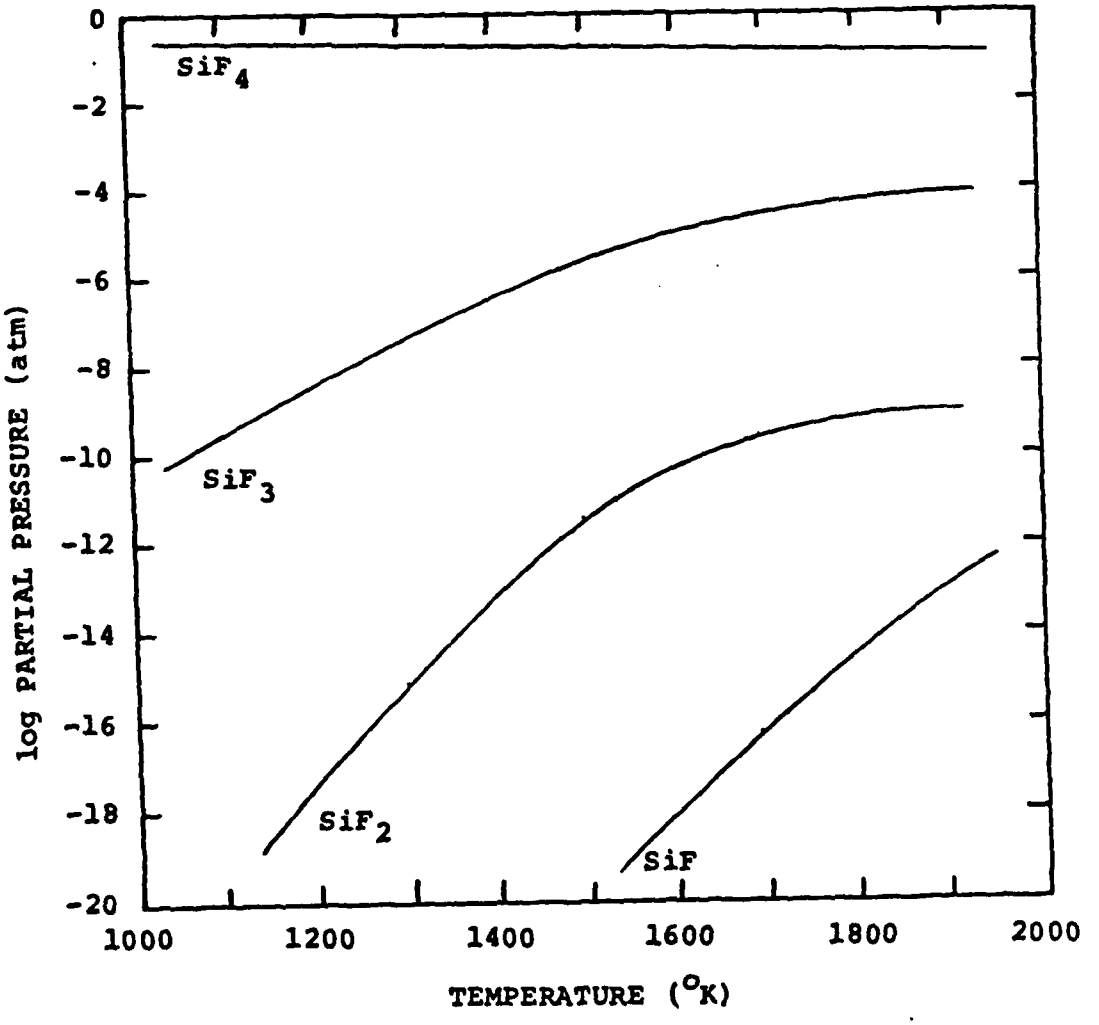

Fig. 6. Log partial pressure versus temperature plot for the SiF_x species in the SiO_2-HF system.

TABLE VII

Typical output for the SiC-H_2O system.

Species	Partial Pressure (atm) 1000 °K	1300 °K	1500 °K	1700 °K
C(g)	0	0	1.9×10^{-17}	1.1×10^{-14}
CH	0	1.3×10^{-18}	1.9×10^{-15}	2.8×10^{-13}
CHO	5.8×10^{-15}	3.7×10^{-10}	4.8×10^{-8}	9.4×10^{-7}
CH_2	9.2×10^{-18}	3.9×10^{-14}	4.2×10^{-12}	7.8×10^{-11}
CH_2O	1.5×10^{-13}	5.1×10^{-10}	1.7×10^{-8}	1.1×10^{-7}
CH_3	4.0×10^{-9}	2.0×10^{-7}	1.0×10^{-6}	1.7×10^{-6}
CH_4	8.2×10^{-2}	7.7×10^{-3}	2.4×10^{-3}	4.0×10^{-4}
CO	1.8×10^{-7}	7.3×10^{-4}	2.8×10^{-2}	2.5×10^{-1}
CO_2	8.8×10^{-15}	1.5×10^{-9}	3.2×10^{-7}	8.3×10^{-6}
SiC(g)	0	0	9.5×10^{-18}	1.5×10^{-14}
Si_2C	0	4.4×10^{-17}	1.6×10^{-13}	1.2×10^{-10}
C_2	0	0	9.0×10^{-20}	1.1×10^{-16}
C_2H	7.8×10^{-19}	4.2×10^{-13}	1.4×10^{-10}	4.7×10^{-9}
C_2H_2	1.3×10^{-9}	6.7×10^{-7}	1.0×10^{-5}	2.9×10^{-5}
C_2H_4	5.2×10^{-7}	1.7×10^{-6}	2.5×10^{-6}	9.5×10^{-7}
C_2H_4O	0	7.2×10^{-19}	4.9×10^{-17}	2.9×10^{-16}
C_2O	0	3.1×10^{-18}	1.7×10^{-14}	4.7×10^{-12}
SiC_2	0	3.0×10^{-17}	1.3×10^{-13}	5.3×10^{-11}
C_3	0	0	4.7×10^{-18}	2.8×10^{-15}
C_3O_2	0	1.1×10^{-18}	9.5×10^{-15}	2.0×10^{-12}
C_4	0	0	0	2.1×10^{-20}
$C_4H_{12}Si$	2.1×10^{-15}	3.5×10^{-18}	1.4×10^{-19}	0
C_5	0	0	0	2.4×10^{-20}
H	2.2×10^{-9}	1.1×10^{-6}	1.7×10^{-5}	1.3×10^{-4}

TABLE VII (CONT.)

OH	2.3×10^{-19}	7.0×10^{-14}	1.8×10^{-11}	9.3×10^{-10}
HO_2	0	0	0	0
SiH	4.6×10^{-18}	1.1×10^{-12}	2.4×10^{-10}	2.0×10^{-8}
H_2	0.918	0.992	0.969	0.748
H_2O	4.5×10^{-8}	4.9×10^{-6}	3.6×10^{-5}	1.1×10^{-4}
H_2O_2	0	0	0	0
SiH_4	2.1×10^{-10}	3.1×10^{-9}	9.2×10^{-9}	1.9×10^{-8}
Ar	0	0	0	0
O	0	7.5×10^{-20}	2.8×10^{-16}	1.3×10^{-13}
SiO	1.0×10^{-12}	4.0×10^{-7}	4.2×10^{-5}	1.8×10^{-3}
O_2	0	0	0	8.1×10^{-18}
SiO_2	0	1.4×10^{-15}	2.0×10^{-12}	5.1×10^{-10}
O_3	0	0	0	0
Si(g)	6.3×10^{-20}	1.2×10^{-13}	7.2×10^{-11}	1.4×10^{-8}
Si_2	0	9.1×10^{-20}	7.0×10^{-16}	1.4×10^{-12}
Si_3	0	0	9.2×10^{-19}	7.7×10^{-15}
Values listed below are molar quantities.				
C(ref)	1.69	1.97	1.81	0
α-SiC	0	0	0	0
β-SiC	8.00	8.00	8.06	8.66
SiO_2(q)	2.00	0	0	0
SiO_2(cr)	0	2.00	1.94	1.33
SiO_2(liq)	0	0	0	0
Si(ref)	0	0	0	0
Si(liq)	0	0	0	0

TABLE VIII

Typical output for the Si_3N_4-H_2O system.

Species	Partial Pressure (atm) 1000 °K	1300 °K	1500 °K	1700 °K
H	2.0×10^{-9}	9.5×10^{-7}	1.5×10^{-5}	1.3×10^{-4}
NH	9.6×10^{-18}	1.2×10^{-13}	7.6×10^{-12}	1.9×10^{-10}
HNO	0	3.8×10^{-18}	4.4×10^{-16}	1.7×10^{-14}
HNO_2(C)	0	0	0	0
HNO_2(T)	0	0	0	1.1×10^{-20}
HNO_3	0	0	0	0
OH	4.0×10^{-16}	3.6×10^{-12}	2.0×10^{-10}	4.3×10^{-9}
HO_2	0	0	0	1.1×10^{-19}
SiH	0	2.7×10^{-16}	1.4×10^{-12}	9.1×10^{-10}
H_2	0.750	0.750	0.750	0.749
NH_2	8.3×10^{-12}	7.6×10^{-10}	6.1×10^{-9}	2.5×10^{-8}
N_2H_2	2.3×10^{-18}	7.0×10^{-16}	8.9×10^{-15}	6.3×10^{-14}
H_2O	7.1×10^{-5}	2.2×10^{-4}	3.5×10^{-4}	5.0×10^{-4}
H_2O_2	0	0	6.4×10^{-20}	0
NH_3	1.9×10^{-4}	4.1×10^{-5}	2.0×10^{-5}	1.2×10^{-5}
N_2H_4	2.7×10^{-18}	3.2×10^{-17}	9.6×10^{-17}	2.3×10^{-16}
SiH_4	3.7×10^{-17}	5.2×10^{-13}	3.6×10^{-11}	8.9×10^{-10}
N	0	8.2×10^{-17}	3.0×10^{-14}	2.7×10^{-12}
NO	3.6×10^{-19}	1.3×10^{-14}	1.4×10^{-12}	5.1×10^{-11}
NO_2	0	0	0	0
NO_3	0	0	0	0
SiN	0	6.5×10^{-17}	3.2×10^{-13}	2.0×10^{-10}
Si_2N	0	0	2.2×10^{-17}	3.7×10^{-13}
N_2	0.250	0.250	0.250	0.250

TABLE VIII (CONT.)

N_2O	0	4.3×10^{-19}	4.4×10^{-17}	1.5×10^{-15}
N_2O_3	0	0	0	0
N_2O_4	0	0	0	0
N_2O_5	0	0	0	0
O	0	4.4×10^{-18}	3.5×10^{-15}	5.9×10^{-13}
SiO	5.3×10^{-15}	6.9×10^{-9}	3.4×10^{-6}	3.8×10^{-4}
O_2	0	0	7.7×10^{-19}	1.8×10^{-16}
SiO_2(g)	0	1.4×10^{-15}	2.0×10^{-12}	5.1×10^{-10}
O_3	0	0	0	0
Si(g)	0	3.5×10^{-17}	4.7×10^{-13}	6.4×10^{-10}
Si_2	0	0	3.0×10^{-20}	2.9×10^{-15}
Si_3	0	0	0	7.3×10^{-19}
Ar	0	0	0	0
Values listed below are molar quantities.				
Si(liq)	0	0	0	0
Si(ref)	0	0	0	0
SiO_2(liq)	0	0	0	0
SiO_2(cr)	0	0.17	0.17	0.16
SiO_2(q)	0.17	0	0	0
α-Si_3N_4	0	0	0	0
Si_2N_2O	3.67	3.67	3.67	3.67

TABLE IX

Effect of decreasing H_2O content on molar quantities of the condensed species in the Si_3N_4-H_2O system.

Species	Moles of Water 4	3	2	1
Si(liq)	0	0	0	0
Si(ref)	0	0	0	0
SiO_2(liq)	0	0	0	0
SiO_2(q)	0	0	0	0
SiO_2(cr)	0.17	0	0	0
α-Si_3N_4	0	0.5	1.17	1.83
Si_2N_2O	3.67	3.00	2.00	1.00

TABLE X

Typical output for the SiO_2-H_2O system.

Species	Partial Pressure (atm) 1000 °K	1300 °K	1500 °K	1700 °K
H	1.1×10^{-12}	5.5×10^{-9}	2.5×10^{-7}	4.6×10^{-6}
OH	9.9×10^{-9}	2.8×10^{-6}	3.5×10^{-5}	2.4×10^{-4}
HO_2	1.9×10^{-14}	3.0×10^{-11}	7.9×10^{-10}	9.6×10^{-9}
SiH	0	0	0	0
H_2	2.5×10^{-7}	2.5×10^{-5}	2.4×10^{-4}	9.7×10^{-4}
H_2O	1.00	1.00	0.999	0.998
H_2O_2	9.5×10^{-13}	1.9×10^{-10}	2.0×10^{-9}	0
SiH_4	0	0	0	0
Ar	0	0	0	0
O	5.4×10^{-14}	6.0×10^{-10}	3.8×10^{-8}	9.1×10^{-17}
SiO	0	5.0×10^{-17}	3.1×10^{-13}	2.4×10^{-10}
O_2	1.2×10^{-7}	1.2×10^{-5}	9.0×10^{-5}	4.2×10^{-4}
SiO_2(g)	0	1.4×10^{-15}	2.0×10^{-12}	5.1×10^{-10}
O_3	0	1.9×10^{-17}	2.3×10^{-15}	9.4×10^{-14}
Si(g)	0	0	0	0
Si_2	0	0	0	0
Si_3	0	0	0	0
Values listed below are molar quantities.				
SiO_2(q)	5.00	0	0	0
SiO_2(cr)	0	5.00	5.00	5.00
SiO_2(liq)	0	0	0	0
Si(ref)	0	0	0	0
Si(liq)	0	0	0	0

TABLE XI

Comparison of free energy minimization data.

System: Si-HCl in Ar
System Pressure: 1 atm
Reaction Temperature: 1600 ^{o}K
Cl:H Ratio: 0.1

Species	Partial Pressure (atm) Gordon-McBride Program*	SOLGASMIX-PV
H_2	0.875	0.870
$SiCl_4$	1.43×10^{-3}	8.57×10^{-4}
$SiHCl_3$	2.46×10^{-3}	2.45×10^{-3}
SiH_2Cl_2	3.07×10^{-4}	1.38×10^{-3}
SiH_3Cl	2.01×10^{-5}	2.63×10^{-2}
SiH_4	9.00×10^{-7}	1.15×10^{-6}
HCl	9.02×10^{-2}	8.82×10^{-2}
$SiCl_3$	4.38×10^{-3}	1.02×10^{-2}
$SiCl_2$	3.30×10^{-2}	2.46×10^{-2}
SiCl	3.14×10^{-6}	5.21×10^{-6}
Cl_2	1.43×10^{-9}	1.37×10^{-9}
Cl	4.14×10^{-6}	4.12×10^{-6}
H	5.03×10^{-5}	5.04×10^{-5}
SiH	2.02×10^{-7}	2.02×10^{-7}
Si	9.36×10^{-8}	9.36×10^{-8}
Si_2	2.49×10^{-10}	2.49×10^{-10}
Si_3	5.53×10^{-11}	5.55×10^{-11}

*C.S. Herrick and R.A. Sanchez-Martinez, "Equilibrium Calculations for the Si-H-Cl System from 300 to 3000 K," J. Electrochem. Soc., 131 [2] 454 (1984).

REFERENCES

1. D.R. Stull and H. Prophet, "JANAF Thermochemical Tables, Second Edition," NBS Publication 37, U.S. Government printing Office, Washington (1971).

2. L.B. Pankratz, "Thermodynamic Properties of Elements and Oxides," U.S. Bureau of Mines Bulletin 672, U.S. Government Printing Office, Washington (1982).

3. C.E. Wicks and F.E. Block, "Thermodynamic Properties of 65 Elements - Their Oxides, Halides, Carbides, and Nitrides," U.S. Bureau of Mines Bulletin 605, U.S. Government Printing Office, Washington (1963).

4. O. Kubachewski and C.B. Alcock, Metallurgical Thermochemistry, Pergamon Press, New York (1979).

5. M. Bruce Fegley, Jr., "The Thermodynamic Properties of Silicon Oxynitride," J. Am. Ceram. Soc. **64** [9] C124 (1981).

6. G. Fischman, "Appendix II," M.S. Thesis, University of Illinois, Urbana, Illinois (1983).

7. R.S. Gordon and B.J. McBride, "Computer Program for Calculation of Complex Chemical Equilibrium Compositions, Rocket Performance, Incident and Reflected Shocks, and Chapman-Jouguet Detonations," NASA Report SP-275, NTIS, Springfield, Virginia (1971).

8. C.S. Herrick and R.A. Sanchez-Martinez, "Equilibrium Calculations for the Si-H-Cl System from 300 to 3000 K," J. Electrochem. Soc. **131** [2] 454 (1984).

9. L.P. Hunt and E. Sirtl, " A Thorough Thermodynamic Evaluation of the Silicon-Hydrogen-Chlorine System," J. Electrochem. Soc. **119** [12] 1741 (1972).

10. M. Farber and R.D. Srivastava, J. Chem. Thermodyn. **11** 939 (1979).

END

FILMED

3-86

DTIC